U.S. Department of Commerce
National Oceanic and Atmospheric Administration
National Weather Service
National Centers for Environmental Prediction
5200 Auth Road
Camp Springs, MD 20746-4304

Office Note 455

GENERALIZED FIBONACCI GRIDS; A NEW CLASS OF STRUCTURED, SMOOTHLY ADAPTIVE MULTI-DIMENSIONAL COMPUTATIONAL LATTICES

R. James Purser*
Science Applications International Corp., Beltsville, Maryland

May 13, 2008

* email: jim.purser@noaa.gov

Abstract

This paper describes ways of extending the spatially-homogeneous two-dimensional computational 'Fibonacci grid' of Swinbank and Purser, and Hannay and Nye, to related grids exhibiting more general patterns of variable resolution and to higher dimensions. In principle, such a grid allows a single unified global computational framework to contain several independent subregions of enhanced resolution, blending smoothly with the rest of the grid where a uniform coarser resolution is maintained. Remarkably, it is able to do this without the geometry of the immediate neighborhood of any grid point (except near its two 'polar' singularities) exhibiting departures larger than a small fixed measure of deformation from a square, or cubic, lattice configuration. For meteorological data assimilation, such a grid has the advantage that the whole global domain's data can be assimilated in a single procedure that automatically accounts for the need to provide higher resolution in locations of special meteorological interest (cyclones, fronts, etc.). It may prove possible to use the new class of grids as the computational frameworks of numerical weather prediction models, in which case, the same advantages of unification carry over into this activity also.

Associated with the higher-dimensional generalizations of these Fibonacci computational lattices we find generalizations, or analogues, of the Fibonacci and Lucas numbers themselves, but these new numbers occupy regular arrays having a dimensionality one less than the dimensionality of the space in which the Fibonacci lattices reside. It is shown that these 'Quasi-Fibonacci' numbers assume roles with respect to the generalized Fibonacci lattices exactly analogous to the roles played by the standard Fibonacci numbers in relation to the two-dimensional Fibonacci lattices, where they determine which generalized lines of the computational lattice can ever become suitable lines along which it is feasible to apply standard numerical operations of finite differencing, integration, filtering and interpolation.

1. Introduction

The 'Fibonacci matrix':

$$\boldsymbol{M} = \begin{bmatrix} 1, & 1 \\ 1, & 0 \end{bmatrix}, \tag{1.1}$$

produces the well-known Fibonacci number series, three consecutive members at a time, as the components of each of the successive powers of $\boldsymbol{M}$. The eigenvalues are, ϕ and $-1/\phi$, where $\{1 : \phi\} = \{\phi - 1 : 1\}$ defines the 'golden ratio', ϕ being the quantity:

$$\phi = \frac{\sqrt{5}+1}{2} \approx 1.618. \tag{1.2}$$

The magnitudes of the components of the eigenvectors are in this ratio and their orthogonal orientations, that is, rotations from the Cartesian directions by an angle,

$$\alpha = \arctan(\phi), \tag{1.3}$$

provide the optimal choice for principal component directions of pure deformations when it is required that the action of arbitrary deformations of this kind lead to no close collisions of the deformed lattice points. This is the crucial condition exploited in the construction of the highly homogeneous two-dimensional (2D) 'Fibonacci grid' of Swinbank and Purser (1999, 2006) and Hannay and Nye (2004). The difference between the homogeneous and the adaptive Fibonacci grids can be characterized by the differences between the two latent frameworks, here called 'skeleton grids', which guide the construction of the Fibonacci grids. In each of the two cases, the skeleton grid is orthogonal and its local coordinate directions are oriented with respect to the associated Fibonacci grid ('F-grid') in such a way that, at points where the F-grid is locally square, the relative orientation between it and the guiding skeleton grid is very close to the angle α defined by (1.3).

If we imagine continuously 'uncurling' the skeleton grid to make it Cartesian and regular, then each of the families of lines of the embedded F-grid also uncurl and become straight, parallel and regular in their spacing. However, in the case of the homogeneous F-grid, the original skeleton grid was envisaged to be formed of uniformly spaced coordinates of an equal-area orthogonal mapping of the horizontal domain. Such a coordinate pair is formed by azimuth and the square-root of radius for the plane, or longitude and sine–latitude for the case of the sphere. The equal-area property was then inherited by the F-grid. In contrast, by allowing the skeleton grid to have variable areal resolution, while remaining very nearly orthogonal, the collision-avoiding property of the associated F-grid (which only depends upon the skeleton grid's orthogonality) is maintained, but it is now the adaptive enhancement of resolution that is inherited by the F-grid.

The adaptive F-grids in two dimensions require, at each grid point, two geographical co-ordinates to be defined. The number of 'unknowns' therefore fortuitously matches the two constraints that we wish to impose at each point: one constraint to maintain orthogonality of the skeleton grid coordinates and the other to specify the desired absolute Jacobian, or areal resolution.

In three dimensions, we are slightly restricted, and must therefore make compromises, in enforcing the constraints we desire since, although there are only three 'unknowns' at each

gridpoint (to specify their location in space) we would ideally wish for the freedom to enforce the three necessary orthogonality constraints *and* the additional specification of the grid's absolute Jacobian. Given that compromises, articulated in the form of a suitable variational principle, will be made in constructing a skeleton grid in 3D, we still must come up with a systematic way of generalizing the crucial properties of the F-grid to three dimensions that will ensure the same kind of guaranteed collision-avoidance amongst the 3D F-grid points that the classical Fibonacci sequence and 'golden ratio' formalism achieved in the case of the 2D F-grid. It is this part of the problem of consistently formulating a 3D (adaptive or homogeneous) F-grid that this note will focus upon. The natural solution to this part of the problem has been found, and is summarized in the following section. While the classical Fibonacci numbers and 'golden ratio' no longer play a role in the 3D formulation, obvious mathematical properties and relationships of the new 'quasi-Fibonacci' numbers (and the analogous ratios associated with a new set, this time, of three eigenvalues) will not fail to be noticed by anyone familiar with the more well-known attributes of the classical Fibonacci and Lucas sequences (e.g., Conway and Guy 1996).

Some of these higher-order quasi-Fibonacci numbers have been studied in the context of aperiodic tiling problems and quasi-crystals that exhibit seven-fold symmetries (Terauchi et al. 1990, Steinbach 1997, Franco 1993) while, in pure mathematics, the quasi-Fibonacci numbers have been generalized in other ways (e.g., Wituła et al. 2006) and found to display numerous intriguing identities with recognizable analogues in the original Fibonacci and Lucas sequences.

2. Definition of orientations

Relative to the 3D Fibonacci lattice when it is cubic, the deformation axes aligned with the skeleton grid can be defined as the eigenvectors of the quasi-Fibonacci matrix, $\boldsymbol{M}_0$:

$$\boldsymbol{M}_0 = \begin{bmatrix} 1, & 1, & 1 \\ 1, & 1, & 0 \\ 1, & 0, & 0 \end{bmatrix}. \tag{2.1}$$

The possible eigenvalues of $\boldsymbol{M}_0$ in the expression,

$$\boldsymbol{M}_0 \boldsymbol{V} = \boldsymbol{V} R \tag{2.2}$$

are given by roots R in the characteristic equation,

$$\det(\boldsymbol{M}_0 - \boldsymbol{I} R) = 0, \tag{2.3}$$

or,

$$R^3 - 2R^2 - R + 1 = 0. \tag{2.4}$$

Applying the standard trigonometric approach to solving the cubic, let $\theta_j, \quad j = 0, 1, 2$ be the three angles in $[0, \pi]$ that satisfy,

$$\cos(3\theta_j) = \frac{1}{2\sqrt{7}}. \tag{2.5}$$

Then, to each such θ_j there is a corresponding root to the characteristic equation of the form:

$$R_j = \frac{2}{3}\left(1 + \sqrt{7}\cos(\theta_j)\right). \tag{2.6}$$

However, as we show in the appendix, by exploiting the special form of the matrix, $\boldsymbol{M}_0$, we can alternatively write the eigenvalues,

$$R_j = \frac{(-1)^j}{2\sin[(2j+1)\pi/14]}, \quad j = 0, 1, 2. \tag{2.7}$$

Either way, the three possibles solutions are:

$$R_0 \approx 2.246979603717467, \tag{2.8a}$$
$$R_1 \approx -0.801937735804838, \tag{2.8b}$$
$$R_2 \approx 0.554958132087372, \tag{2.8c}$$

and the corresponding eigenvectors can be taken as the columns of the symmetric orthogonal matrix,

$$\boldsymbol{V} = \begin{bmatrix} v_0, & v_1, & -v_2 \\ v_1, & v_2, & -v_0 \\ -v_2, & -v_0, & v_1 \end{bmatrix}, \tag{2.9}$$

where,

$$v_0 = \frac{2}{\sqrt{7}}\cos(\pi/14) \approx 0.7369762290995780, \tag{2.10a}$$
$$v_1 = \frac{2}{\sqrt{7}}\cos(3\pi/14) \approx 0.5910090485061035, \tag{2.10b}$$
$$v_2 = \frac{2}{\sqrt{7}}\cos(9\pi/14) \approx -0.3279852776056819. \tag{2.10c}$$

Assuming modulo-3 arithmetic on the index, α, we find that:

$$v_\alpha = \frac{1}{R_{\alpha+2} - R_{\alpha+1}}, \tag{2.11}$$

and that

$$R_\alpha = -\frac{v_\alpha}{v_{\alpha-1}}. \tag{2.12}$$

We define a matrix, $\boldsymbol{P}$, that denotes the signed-permutation of the coordinate basis:

$$\boldsymbol{P} = \begin{bmatrix} 0, & 0, & -1 \\ 1, & 0, & 0 \\ 0, & -1, & 0 \end{bmatrix} \tag{2.13}$$

and, from the cyclic pattern of the eigenvectors, $\boldsymbol{V}$, we find that the application of $\boldsymbol{P}$ to $\boldsymbol{V}$ preserves, but cyclically rotates, the sequence of columns with sign-changes that preserve matrix symmetry:

$$\boldsymbol{PV} = \begin{bmatrix} v_2, & v_0, & -v_1 \\ v_0, & v_1, & -v_2 \\ -v_1, & -v_2, & v_0 \end{bmatrix}, \tag{2.14}$$

and again:

$$\boldsymbol{P}^2\boldsymbol{V} = \begin{bmatrix} v_1, & v_2, & -v_0 \\ v_2, & v_0, & -v_1 \\ -v_0, & -v_1, & v_2 \end{bmatrix}. \tag{2.15}$$

The same repeated orthogonal transformation therefore produces two independent matrices similar to $\boldsymbol{M}_0$ that must mutually commute (since they share the same eigenvectors):

$$\boldsymbol{M}_1 \equiv \boldsymbol{P}\boldsymbol{M}_0\boldsymbol{P}^{-1} = \begin{bmatrix} 0, & -1, & 0 \\ -1, & 1, & -1 \\ 0, & -1, & 1 \end{bmatrix}, \tag{2.16a}$$

$$\boldsymbol{M}_2 \equiv \boldsymbol{P}^2\boldsymbol{M}_0\boldsymbol{P}^{-2} = \begin{bmatrix} 1, & 0, & -1 \\ 0, & 0, & 1 \\ -1, & 1, & 1 \end{bmatrix}. \tag{2.16b}$$

The significance of finding such commuting integer-component matrices is that, if an initially cubic lattice alligned with Cartesian coordinates is subjected to a pure linear deformation whose principal axes coincide with the orientation expressed in this Cartesian coordinate system by the eigenvectors, and if the dilatation components are proportional to the logarithms of the absolute values of the eigenvalues, then, after a finite lapse of time, the deformed lattice comes into a new configuration which is also a perfect cubic lattice and which is the mirror image in one of the coordinate planes of the original lattice. After a further equal lapse of time under the same constant deformation conditions, the lattice transforms to another perfectly cubic configuration, and this time the lattice points exactly coincide with the original lattice points.

A cyclic rotation of the three deformation principal components leads to three completely different deformation operators, but each has the same property of returning the initially cubic lattice periodically to new cubic lattices that alternate between the original configuration and a mirror image of it. There is a sense, which can be expressed rigorously, in which the 'distance' of the deformed lattice from its original cubic configuration never exceeds a definite quantifiable bound, even when arbitrary amounts of the 'allowed' (commuting) deformation operators are applied. Pathological lattice configurations cannot occur where, along lines or within planes, distances between the adjacent lattice point become very much closer than between these lines or planes themselves. In effect, each member of the commuting set of general deformations defines a point in a Euclidean deformation space in which the metric 'distance'-squared between two deformation operators, A and B is just the sum of the squares of the logarithms of the eigenvalues of the combination $A^{-1}B$ or, equivalently, $B^{-1}A$. Restricting attention to unit-determinant deformations so as not to complicate the picture with considerations of overall scale, the 'points' in deformation space at which the originally cubic grid becomes cubic once again, is itself a regular lattice and no point in deformation space is a greater distance from one of the 'cubic' points than the largest radius of the representative Voronoi cell of this two-dimensional deformation-space lattice. (The Voronoi cell of a regular lattice is the set of points closer to the central lattice point than to any other lattice point. For example, see Preparata and Shamos, 1985.)

The effect of applying generic eigenvector-aligned deformations is produced in practice by building up the generalized Fibonacci grid as a perfectly regular lattice within the coordinate

framework supplied by an arbitrarily defined smooth orthogonal coordinate system. In the original Fibonacci grid defined by Swinbank and Purser (1999, 2006) this skeleton coordinate system was implicit – simply the ordinary orthogonal system of sine-latitude and longitude whose areal resolution is perfectly uniform on the spherical surface. However, it is possible to generate a vast range of less trivial skeleton coordinate systems which can be made visible by plotting their associated grids of lines at equal coordinate increments. When the Fibonacci lattice is embedded within such a grid and shares the relative deformations of the skeleton grid across regions where the aspect ratio of the unit increments of the skeleton framework is changing, the embedded Fibonacci grid shares this same deformation. But, as a result of the special alignment it has relative to the skeleton grid's coordinate directions, it never suffers the pathologies of grid-point near-collisions. In fact, as we have indicated, it can never be very far away (in the sense of the deformation metric) from a locally square grid.

The two-dimensional case is easier to illustrate than one in higher dimensions. In Fig. 1 a two-dimensional curvilinear, but approximately orthogonal, polar grid is constructed over a portion of the Euclidean plane containing three distinct regions where enhanced resolution is prescribed: an elongated elliptical region to the 'west' with a mild enhancement, and a pair of approximately circular regions of stronger enhancement located north-east and south of the 'pole' of the coordinate system. The enhancement is measured by the areal resolution of the skeleton coordinate system (i.e., by its Jacobian) and it is quite immaterial how large the local aspect ratio of the skeleton grid becomes. This point is important because, in general, we should *not* expect the skeleton coordinate system itself to be remotely suitable as a numerical modeling framework. Nevertheless, regardless of how extremely 'deformed' it appears locally, the Fibonacci grid embedded within it retains the local appearance everywhere of a smooth and well-proportioned curvilinear grid.

The generalized Fibonacci lattice associated with the skeleton grid of Fig. 1 is shown in Fig. 2 and the arrangement, apart from the inevitable irregularities near the 'pole' (where special numerical treatment are always needed; Swinbank and Purser 2006) shows that the Fibonacci grid does indeed succeed in providing the desired degree of enhancement of the resolution in the three specified regions while retaining smooth continuity throughout. The square box where the high density of grid points obscures their gridded arrangement is shown expanded in Fig. 3 and another subregion of that figure is given a further enlargement in Fig. 4, where it is especially striking how smooth and regular the enhanced grid seems, even within the region of maximum resolution.

To summarize, a system of $n-1$ mutually commuting and multiplicatively independent integer-component symmetric matrices with shared eigenvectors aligned obliquely to the basic Cartesian directions guarantees the existence of an associated generalized 'Fibonacci'-type grid having the areal or volumetric resolution proportional to that of any given orthogonal 'skeleton' coordinate system spanning the domain of interest. Extreme aspect ratios inherent to the skeleton system are *not* inherited by the embedded 'Fibonacci'-type lattice because the $n-1$ dimensional space of possible unimodular deformations that share the oblique eigenvectors contains a lattice of deformation points, corresponding to where the Fibonacci grid is exactly square, cubic or hyper-cubic, which makes it impossible for any given deformation of the prescribed kind to be farther than a known fixed 'distance' from one of these cubic-configuration lattice points.

The question of how a suitable skeleton system can be constructed to provide the intended resolution enhancements is one that deserves a separate technical discussion and is not further considered here. Instead, we explore some of the algebraic and geometrical properties of the particular $n = 3$-dimensional example of the generalized Fibonacci grid which forms the main focus of this study.

3. Identities connecting the eigenvalues, R_α, and the 'quasi-Fibonacci' numbers

The R are connected by various identities, a sample of which are as follows:

$$\begin{aligned} R_{\alpha-1} &= -2R_\alpha + R_\alpha^2, && \text{(3.1a)} \\ &= \frac{R_\alpha}{R_\alpha^2 - 1}, && \text{(3.1b)} \\ &= \frac{R_\alpha - 1}{R_\alpha}. && \text{(3.1c)} \\ & && \text{(3.1d)} \end{aligned}$$

From the first of these it is evident that an algebraic expression comprising a sum of terms whose factors are all integer multiples of arbitrary integer powers of R_0, R_1, R_2, can be reduced to sums of powers of just one of them, R_0, say. Moreover, since the characteristic equation can be used iteratively to reduce each exponent of R_0 to either: zero, one, or two, the general power expansion is reduced to an integer-coefficient quadratic. We see how this works by considering simple powers of R_0 itself. The following equations establish a simple recursive pattern:

$$\begin{aligned} R_0^0 &= 1 + 0R_0 + 0R_0^2, && \text{(3.2a)} \\ R_0^1 &= 0 + 1R_0 + 0R_0^2, && \text{(3.2b)} \\ R_0^2 &= 0 + 0R_0 + 1R_0^2, && \text{(3.2c)} \\ R_0^3 &= -1 + 1R_0 + 2R_0^2, && \text{(3.2d)} \\ R_0^4 &= -2 + 1R_0 + 5R_0^2, && \text{(3.2e)} \\ R_0^5 &= -5 + 3R_0 + 11R_0^2, && \text{(3.2f)} \end{aligned}$$

and so on. If we write the generic terms,

$$R_0^p = f_{(0)p} + f_{(1)p}R_0 + f_{(2)p}R_0^2, \tag{3.3}$$

we find that each of the three types of coefficient, f, obeys the same recurrence:

$$f_p - 2f_{p-1} - f_{p-2} + f_{p-3} = 0, \tag{3.4}$$

which mirrors the form of the characteristic equation (2.4). We could perform the expansions of the powers of the other two roots, R_1 and R_2, in exactly the same way, of course. However, it is more interesting to expand the powers of, say, R_2, but expressed as quadratics of R_0:

$$\begin{aligned} R_2^0 &= 1 + 0R_0 + 0R_0^2, && \text{(3.5a)} \\ R_2^1 &= 0 - 2R_0 + 1R_0^2, && \text{(3.5b)} \end{aligned}$$

$$R_2^2 = 2 - 3R_0 + 1R_0^2, \tag{3.5c}$$
$$R_2^3 = 3 - 8R_0 + 3R_0^2, \tag{3.5d}$$
$$R_2^4 = 8 - 17R_0 + 6R_0^2, \tag{3.5e}$$
$$R_2^5 = 17 - 39R_0 + 14R_0^2, \tag{3.5f}$$

and so on.

Note that the each member of the trio of successive coefficients in this sequence obeys precisely the same recurrence as before. In both series, applying the recursion in the negative direction establishes equally valid formulas for the reciprocal powers of R_0 or of R_2. Owing to linearity in the recurrence relations it is also possible to build up a lattice of identities defining each mixed combination of powers of both R_0 and R_2 together, each as a quadratic expression in R_0. When this is done, we see that the expressions collectively manifest a great deal of redundancy, with the same numerical coefficients reappearing in the expressions for several terms. Some of this redundancy is already evident in the sequences for simples powers of R_0 and R_2 above. It turns out that a *single* array will suffice to provide all the needed coefficients and, with appropriate sign changes, for the corresponding expansions of powers of R_1 in terms of the R_0.

The natural pattern made by the coefficients in their most symmetrical arrangement is an equilateral-triangular, or 'hexagonal' lattice. There is a three-fold symmetry exhibited by the pattern formed by the magnitudes of these numbers. This symmetry is reproduced in the indices of the tabulated entries when we deliberately introduce the redundancy of requiring *three* indices for each entry (although two are formally enough to define each number uniquely). The numerical values, which in many ways form higher dimensional generalization of the classical Fibonacci sequence, are therefore each denoted, $F_{i,j,k}$, referred to collectively as 'F-numbers', or 'quasi-Fibonacci numbers', and their triple-indices are subject to the 'zero sum' consistency condition:

$$i + j + k = 0, \tag{3.6}$$

together with a modulo-3 'cyclic offset':

$$j - i \equiv k - j \equiv i - k = 1 \bmod 3. \tag{3.7}$$

The absolute magnitudes of the numbers $F_{i,j,k}$ are symmetrical under cyclic permutations of the indices, but their signs vary in accordance with:

$$F_{i,j,k} = (-)^j F_{j,k,i}. \tag{3.8}$$

The quadratic polynomials of R_α, representing simple powers jointly of R_α and $R_{\alpha-1}$, and whose coefficients are found in the infinite array of these F, are each denoted $\mathcal{F}_{i,j,k}(R_\alpha)$, where the zero-sum condition, (3.6), is maintained (as it is for all indexed quantities discussed in this note), but the cyclic offset condition for the polynomials, $\mathcal{F}_{i,j,k}$, is:

$$j - i \equiv k - j \equiv i - k = 0 \bmod 3. \tag{3.9}$$

The definition of each $\mathcal{F}$ in terms of the quasi-Fibonacci numbers F is

$$\mathcal{F}_{i,j,k}(R_\alpha) = -F_{i-3,j+1,k+2} + F_{i-4,j+3,k+1}R_\alpha + F_{i-1,j,k+1}R_\alpha^2. \tag{3.10}$$

Tabulated values of the F for a fairly small hexagonal patch of index combinations centered on the origin (marked by an asterisk) are shown in Fig. 5. The index i is a measure of the location relative to the origin in the 'compass direction' 90°, contours of constant i therefore run along directions 0°–180°. Index j measures the same distance but in the 210° direction, contours of j running 120°–300°. Finally, the third (and formally redundant) index, $k = -i - j$ measures displacement in the direction, 330° with contours of k running 60°–240°. The 'index point', $\boldsymbol{i} = (i, j, k)$, of the polynomial (3.10) is therefore positioned at the lower-right corner of the hexagonal cell in Fig. 5 that contains the polynomial's third coefficient.

With these tabulated values, we may inductively verify that the coefficient for the general term formed by powers of R_α and $R_{\alpha-1}$ is defined by,

$$R_\alpha^p R_{\alpha-1}^q = \mathcal{F}_{i+2p-q,j-p+2q,k-p-q}(R_\alpha). \tag{3.11}$$

Now consider the polynomial expression for $R_{\alpha+1}$ in terms of R_α. Applying (3.1a) twice and employing the characteristic equation to convert third and fourth power terms to combinations of lower powers, we find that:

$$R_{\alpha+1} = 2 + R_\alpha - R_\alpha^2. \tag{3.12}$$

Inspection of the numbers in Fig. 5, together with the index definitions, reveals that:

$$-R_{\alpha+1} = \mathcal{F}_{-1,-1,2}(R_\alpha). \tag{3.13}$$

Thus, we see that powers of the basic root, R_α, form quadratic polynomials in R_α that march progressively away from the origin of the array of F-numbers array in the positive i-index direction; powers of $R_{\alpha-1}$ form polynomials in R_α that march away from the origin in the j-index direction; powers of $-R_{\alpha+1}$ form polynomials in R_α that march away from the origin in the k-index direction. Moreover, it is clear from the algebraic linearity of the these recurrences that they must remain equally valid for powers that are negative integers. It is tempting to conjecture that *any* rational-coefficient algebraic expression in combinations jointly of the R_0, R_1 and R_2 can be reduced to a unique rational-coefficient quadratic polynomial in any one of these roots. In order to make the assertion evident, we must first reveal some additional identities and relationships among the F-numbers and their generalizations.

We have deduced from the cyclic pattern made by the components of its eigenvectors, $\boldsymbol{V}$, that the matrix $\boldsymbol{M}_0$ shares these eigenvectors with, and therefore commutes with, the similar matrix, $\boldsymbol{M}_2$. When we look at powers of $\boldsymbol{M}_0$ and of $\boldsymbol{M}_2$, and combinations of them, in the context of the tableau of F-numbers, an obvious pattern emerges: each such matrix is encoded by a triangular pattern of the F-numbers in the following way. We define the matrix $[F]_{i,j,k}$, indices subject to (3.6), and the same offset condition (3.9), by:

$$[F]_{i,j,k} = \begin{bmatrix} F_{i+2,j,k-2}, & F_{i+1,j-1,k}, & F_{i,j+1,k-1} \\ F_{i+1,j-1,k}, & F_{i,j-2,k+2}, & F_{i-1,j,k+1} \\ F_{i,j+1,k-1}, & F_{i-1,j,k+1}, & F_{i-2,j+2,k} \end{bmatrix}. \tag{3.14}$$

Then

$$\boldsymbol{I} \equiv [F]_{0,0,0}, \tag{3.15a}$$

$$\boldsymbol{M}_0 \equiv [F]_{2,-1,-1}, \tag{3.15b}$$

$$\boldsymbol{M}_0^2 \equiv [F]_{4,-2,-2}, \tag{3.15c}$$

$$\boldsymbol{M}_2 = -2\boldsymbol{M}_0 + \boldsymbol{M}_0^2 \equiv [F]_{-1,2,-1}. \tag{3.15d}$$

Thus, associating the 'index point' of each such matrix with the central point of its triangular configuration within the tableau, we find a perfect algebraic match between each matrix $[F]_{i,j,k}$ and the corresponding polynomial, $\mathcal{F}_{i,j,k}$, where the elementary polynomial, $\mathcal{F}(R_\alpha) = R_\alpha$, stands in for the basic matrix $\boldsymbol{M}_0$, and the polynomial that describes $R_{\alpha+2}$ in terms of R_α becomes exactly the same polynomial that describes $\boldsymbol{M}_2$ in terms of $\boldsymbol{M}_0$. To complete the correspondence, we should define:

$$\boldsymbol{M}_1 = 2\boldsymbol{I} + \boldsymbol{M}_0 - \boldsymbol{M}_0^2, \tag{3.16}$$

whose polynomial is exactly the one that expresses $R_{\alpha+1}$ in terms of R_α.

The inverses of these matrices can now be read straight from the F-number array and are:

$$\boldsymbol{M}_0^{-1} = \begin{bmatrix} 0, & 0, & 1 \\ 0, & 1, & -1 \\ 1, & -1, & 0 \end{bmatrix}, \tag{3.17a}$$

$$\boldsymbol{M}_1^{-1} = \begin{bmatrix} 0, & -1, & -1 \\ -1, & 0, & 0 \\ -1, & 0, & 1 \end{bmatrix}, \tag{3.17b}$$

$$\boldsymbol{M}_2^{-1} = \begin{bmatrix} 1, & 1, & 0 \\ 1, & 0, & 1 \\ 0, & 1, & 0 \end{bmatrix}. \tag{3.17c}$$

In general, we now see that the matrix formed as the product of arbitrary integer powers of $\boldsymbol{M}_0$, $\boldsymbol{M}_1$ and $\boldsymbol{M}_2$ can be expressed in our F-number notation:

$$\boldsymbol{M}_0^p \boldsymbol{M}_1^q \boldsymbol{M}_2^r = (-)^q [F]_{2p-q-r,2r-p-q,2q-p-r}. \tag{3.18}$$

The set of six matrices $\boldsymbol{M}_\alpha$ and $\boldsymbol{M}_\alpha^{-1}$ may be considered to be equidistant from the identity matrix $\boldsymbol{I}$ in the following sense. As defined in Purser (2005), there is a natural distance measure, s, between any two symmetric matrices $\boldsymbol{A}$ and $\boldsymbol{B}$ of a given order, where s^2 is the sum of the squares of the logarithms of the absolute magnitudes of the eigenvalues of $\boldsymbol{A}^{-1}\boldsymbol{B}$. In general, the metric space thus defined is one exhibiting negative curvature on most geodesic 2-surfaces, but an exception occurs for the cases in which such 2-surfaces correspond to a subset of the matrices sharing the same eigenvectors, and therefore commuting. In this special case, which corresponds to the situation we are dealing with, the geometry implied by the metric is Euclidean. In fact, the arrangement provided by the tabulated F-numbers of Fig. 5, with its 60° regular hexagonal grid, precisely reflects the correct geometrical relationships among the matrices represented here.

Other curious regularities inherent in the arrangement of F-numbers are evident. A 3-vector $\{F\}_{i,j,k}$ can be formed according to the rule:

$$\{F\}_{i,j,k} = (F_{i+1,j,k-1}, F_{i,j-1,k+1}, F_{i-1,j+1,k})^T \tag{3.19}$$

with the index cyclic-offset for these vectors:

$$j - i \equiv k - j \equiv i - k = 2 \bmod 3. \tag{3.20}$$

Notice that the set of components forms a 2-high 'ball stack' in the F-numbers table, oriented in the same sense as the stacks formed by matrices. It is readily verified that these vectors conform to a simple and natural definition for dot-products:

$$\{F\}_{i,j,k} \cdot \{F\}_{i',j',k'} = F_{i+i',j+j',k+k'}, \tag{3.21}$$

and for the product of a matrix with a vector:

$$[F]_{i,j,k}\{F\}_{i',j',k'} = \{F\}_{i+i',j+j',k+k'}. \tag{3.22}$$

We also notice that, since three ordered eigenvalues suffice to define any matrix belonging to the equivalence class that commutes with the set sharing the same eigenvectors, then any three linearly independent matrices of the kind $[F]$ are sufficient as a basis to construct any matrix in the equivalence class. We have already seen how a basis consisting of $\boldsymbol{I}$, $\boldsymbol{M}_0$ and $\boldsymbol{M}_0^2$ forms a quadratic polynomial that expresses the other commuting matrices we have looked at; we now see that this is a general property. However, if the description of each symmetric matrix in the equivalence class can be given by just three coefficients, then, in addition to the trivial requirement of symmetry, each such matrix must additionally possess three linear relationships among its components. It is not too hard to find that these additional conditions are supplied by the following expressions for the off-diagonal matrix elements in terms of the diagonal ones:

$$\begin{aligned} H_{2,3} &= H_{1,1} - H_{2,2}, & (3.23a)\\ H_{1,3} &= H_{2,2} - H_{3,3}, & (3.23b)\\ H_{1,2} &= H_{1,1} - H_{3,3}, & (3.23c) \end{aligned}$$

or, in terms of the F-numbers themselves:

$$\begin{aligned} F_{i,j,k} &= F_{i+3,j,k-3} - F_{i+1,j-2,k+1}, & (3.24a)\\ &= F_{i,j-3,k+3} - F_{i-2,j+1,k+1}, & (3.24b)\\ &= F_{i+1,j+1,k-2} - F_{i-3,j+3,k}. & (3.24c) \end{aligned}$$

By the repeated use of the recurrences, (3.24a)–(3.24c), we can deduce the numbers in one part of an array of F-numbers, or generalizations of them conforming to the same recurrence rules, from a suitably independent set in another part of the array. In particular, for a quadratic polynomial whose three coefficients, f_p, correspond to the one denoted $\mathcal{F}_{i,j,k}$, we can formally verify that the components of the associated matrix, $[F]_{i,j,k}$ really are given by

$$\begin{aligned} [F]_{i,j,k} &= f_0\boldsymbol{I} + f_1\boldsymbol{M}_0 + f_2\boldsymbol{M}_0^2,\\ &= \begin{bmatrix} f_0 + f_1 + 3f_2, & f_1 + 2f_2, & f_1 + f_2\\ f_1 + 2f_2, & f_0 + f_1 + 2f_2, & f_2\\ f_1 + f_2, & f_2, & f_0 + f_2 \end{bmatrix}. & (3.25) \end{aligned}$$

4. Division algebra for polynomials and the generalized quasi-Fibonacci numbers

It is convenient to adopt the algebraic shorthand ('L-notation') for a term such as $A = a_0 f_0 + a_1 f_1 + a_2 f_2$ and the products of such terms, by grouping the coefficients into an '**L**' of the appropriate size:

$$A \equiv \underline{\left| \begin{array}{ll} a_1 & \\ a_2, & a_0 \end{array} \right.} \; . \tag{4.1}$$

Then, if $C = AB$, and $C = c_{00} f_0^2 + c_{11} f_1^2 + c_{22} f_2^2 + c_{12} f_1 f_2 + c_{02} f_0 f_2 + c_{01} f_0 f_1$, we can write:

$$\begin{aligned} C \;\; &\equiv \;\; \underline{\left| \begin{array}{lll} c_{11} & & \\ c_{12}, & c_{01} & \\ c_{22}, & c_{02}, & c_{00} \end{array} \right.} \; , \\ &= \;\; \underline{\left| \begin{array}{ll} a_1 & \\ a_2, & a_0 \end{array} \right.} \; * \underline{\left| \begin{array}{ll} b_1 & \\ b_2, & b_0 \end{array} \right.} \; , \end{aligned}$$

with the coefficients b expressing the quantity, B, and symbol, '$*$', denoting the convolution of the two coefficient arrays so that,

$$\begin{aligned} c_{00} &= a_0 b_0, \\ c_{11} &= a_1 b_1, \\ c_{22} &= a_2 b_2, \\ c_{12} &= a_1 b_2 + a_2 b_1, \\ c_{02} &= a_0 b_2 + a_2 b_0, \\ c_{01} &= a_0 b_1 + a_1 b_0. \end{aligned}$$

Using L-notation, the matrix $[F]_{i,j,k}$ in (3.25) that corresponds to the polynomial $\mathcal{F}_{i,j,k}(R) \equiv f_0 + f_1 R + f_2 R^2$ can be written (dropping the indices, i, j, k, for brevity):

$$[F] \equiv \left[\begin{array}{lll} \underline{\left| \begin{array}{ll} 1 & \\ 3, & 1 \end{array} \right.} \; , & \underline{\left| \begin{array}{ll} 1 & \\ 2, & 0 \end{array} \right.} \; , & \underline{\left| \begin{array}{ll} 1 & \\ 1, & 0 \end{array} \right.} \\ \underline{\left| \begin{array}{ll} 1 & \\ 2, & 0 \end{array} \right.} \; , & \underline{\left| \begin{array}{ll} 1 & \\ 2, & 1 \end{array} \right.} \; , & \underline{\left| \begin{array}{ll} 0 & \\ 1, & 0 \end{array} \right.} \\ \underline{\left| \begin{array}{ll} 1 & \\ 1, & 0 \end{array} \right.} \; , & \underline{\left| \begin{array}{ll} 0 & \\ 1, & 0 \end{array} \right.} \; , & \underline{\left| \begin{array}{ll} 0 & \\ 1, & 1 \end{array} \right.} \end{array} \right] . \tag{4.2}$$

In order to invert this matrix, say $[G] \equiv [F]^{-1}$, we first obtain the matrix $[C]$, of signed cofactors:

$$[C] = \begin{bmatrix} \begin{vmatrix} 0 & & \\ 1, & 1 & \\ 1, & 3, & 1 \end{vmatrix}, & \begin{vmatrix} 0 & & \\ 0, & -1 & \\ -1, & -2, & 0 \end{vmatrix}, & \begin{vmatrix} -1 & & \\ -2, & -1 & \\ 0, & -1, & 0 \end{vmatrix} \\ \begin{vmatrix} 0 & & \\ 0, & -1 & \\ -1, & -2, & 0 \end{vmatrix}, & \begin{vmatrix} -1 & & \\ -1, & 1 & \\ 2, & 4, & 1 \end{vmatrix}, & \begin{vmatrix} 1 & & \\ 2, & 0 & \\ -1, & -1, & 0 \end{vmatrix} \\ \begin{vmatrix} -1 & & \\ -2, & -1 & \\ 0, & -1, & 0 \end{vmatrix}, & \begin{vmatrix} 1 & & \\ 2, & 0 & \\ -1, & -1, & 0 \end{vmatrix}, & \begin{vmatrix} 0 & & \\ 1, & 2 & \\ 2, & 5, & 1 \end{vmatrix} \end{bmatrix}. \tag{4.3}$$

From the inner product of any line of $[F]$ with the corresponding line from $[C]$ we obtain the determinant, D:

$$D = \begin{vmatrix} -1 & & & \\ -2, & -1 & & \\ 1, & 1, & 2 & \\ 1, & 5, & 6, & 1 \end{vmatrix}. \tag{4.4}$$

From the coefficients of the matrix inverse, $[G] = [C]/D$, we can recover the three coefficients, g_0, g_1, g_2, of the quadratic polynomial that corresponds to it:

$$\begin{aligned} (g_0, g_1, g_2) &= [G_{3,3} - G_{2,3}, G_{1,3} - G_{2,3}, G_{2,3}], \\ &= \frac{1}{D} \begin{bmatrix} \begin{vmatrix} -1 & & \\ -1, & 2 & \\ 3, & 6, & 1 \end{vmatrix}, & \begin{vmatrix} -2 & & \\ -4, & -1 & \\ 1, & 0, & 0 \end{vmatrix}, & \begin{vmatrix} 1 & & \\ 2, & 0 & \\ -1, & -1, & 0 \end{vmatrix} \end{bmatrix}. \end{aligned} \tag{4.5}$$

These results allow us to reformulate any finite rational expression in one of the roots, R_α as a quadratic polynomial in R_α. We have already seen that the inverses of the eigenvector components are expressible as differences of the R_α, and hence as quadratics in one of these roots. For example, in terms of R_0:

$$\frac{1}{v_0} = -2 - 3R_0 + 2R_0^2, \tag{4.6a}$$

$$\frac{1}{v_1} = 0 + 3R_1 - 1R_1^2, \tag{4.6b}$$

$$\frac{1}{v_2} = +2 + 0R_1 - 1R_1^2. \tag{4.6c}$$

While none of these polynomials is to be found within the existing array of quasi-Fibonacci numbers, F, we can employ the recurrences implied by (3.23a)–(3.23c) to *construct* a table of 'generalized quasi-Fibonacci' numbers for each of (4.6a), (4.6b) and (4.6c) so that the respective polynomial will be found within its own table. However, rather than constructing three distinct

tables in this manner, we find that, apart from sign changes, all three tables of the new numbers, which we shall call F'-numbers, are equivalent. Moreover, these numbers also exhibit a three-fold symmetry of their magnitudes about the suitably chosen origin. In this case, the cyclic-offset condition for the indices of $F'_{i,j,k}$, becomes:

$$j - i \equiv k - i \equiv i - k = 2 \bmod 3. \tag{4.7}$$

The same sign-switching rule, (3.8), continues to hold. Fig. 6 shows a hexagonal patch of the F'-numbers. We find that, in terms of their associated polynomials, $\mathcal{F}'(R_1)$, the reciprocals of the eigenvector components are symmetrically arranged around the origin:

$$\frac{1}{v_0} = \mathcal{F}'_{-1,0,1}(R_0), \tag{4.8a}$$

$$\frac{1}{v_1} = \mathcal{F}'_{0,1,-1}(R_0), \tag{4.8b}$$

$$\frac{1}{v_2} = -\mathcal{F}'_{1,-1,0}(R_0). \tag{4.8c}$$

Now consider the eigenvector components themselves. When we apply the formula for the determinant, D, to the polynomial for $1/v_0$, with coefficients, $(2, 3, -2)$, we find that $D = 7$. Consequently, applying the formulae for the inverse coefficients, we find that $(g_0, g_1, g_2) = (1, 4, -3)/7$. In a similar manner, we may determine quadratic polynomial expressions for v_2 and v_3. These may be summarized together:

$$v_0 = \frac{1}{7}(-1 - 4R_0 + 3R_0^2), \tag{4.9a}$$

$$v_1 = \frac{1}{7}(\ 3 + 5R_0 - 2R_0^2), \tag{4.9b}$$

$$v_2 = \frac{1}{7}(\ 5 - 1R_0 - 1R_0^2). \tag{4.9c}$$

In fact, it is apparent that all the determinants associated with the matrices contained in the array of F'-numbers are ± 7 and so it is natural to seek a third array of generalized F-numbers, which we shall call the F''-numbers, in which we can find seven-times the inverses of polynomials or matrices of the F'-numbers. This third class of generalized quasi-Fibonacci numbers is displayed in Fig. 7, where we find the polynomials describing v_α to be, in the natural extension of our notation:

$$v_0 = \frac{1}{7}\mathcal{F}''_{1,0,-1}(R_0), \tag{4.10a}$$

$$v_1 = \frac{1}{7}\mathcal{F}''_{0,-1,1}(R_0), \tag{4.10b}$$

$$v_2 = -\frac{1}{7}\mathcal{F}''_{-1,1,0}(R_0). \tag{4.10c}$$

Note that the indices of the F''-numbers conform to the cyclic-offset condition that complements those that characterize the F- and F'-numbers. That is, for the numbers, $F''_{i,j,k}$, we have:

$$j - i \equiv k - j \equiv i - k = 0 \bmod 3, \tag{4.11}$$

and the numbers themselves continue to satisfy the same sign-switching rule, (3.8).

The F'- and F''-numbers, being the simplest and most symmetrical of the generalized quasi-Fibonacci numbers, are somewhat analogous in their relationship to the F-numbers, to the way the classical Lucas sequence of numbers relate to the true Fibonacci numbers. With the inclusion of the F'- and F''-numbers, their vectors, matrices and quadratic polynomials, we note that the following generic multiplication rules, are satisfied for the quantities written '(F)', '(F')' and '(F'')', whether the multiplication symbol, '$\times$' be interpreted as polynomial products, matrix–matrix products, matrix–vector products or vector–vector dot-products:

$$(F) \times (F) \rightarrow (F), \tag{4.12a}$$
$$(F) \times (F') \rightarrow (F'), \tag{4.12b}$$
$$(F) \times (F'') \rightarrow (F''), \tag{4.12c}$$
$$(F') \times (F') \rightarrow (F''), \tag{4.12d}$$
$$(F') \times (F'') \rightarrow 7(F), \tag{4.12e}$$
$$(F'') \times (F'') \rightarrow 7(F'), \tag{4.12f}$$

and the three positional indices always add. Thus, the number of primes in the product-type is the sum, modulo–3, of the primes in the factor-types, and a numerical factor of 7 is put in every time an accumulation of three primes in the product is discarded.

The determinants of the matrices in the numbers systems F, F' and F'' are respectively ± 1, ± 7 and $\pm 7^2$. The trace of each matrix satisfies the following relations:

$$\text{trace}[F]_{i,j,k} = F''_{i,j,k}, \tag{4.13a}$$
$$\text{trace}[F']_{i,j,k} = 7F_{i,j,k}, \tag{4.13b}$$
$$\text{trace}[F'']_{i,j,k} = 7F'_{i,j,k}. \tag{4.13c}$$

5. Associated geometrical relationships

The quasi-Fibonacci numbers are arranged in Figs. 5–7 so that multiplication of their matrices, normalized to unimodularity, corresponds to addition of their indices. These indices therefore serve to map out the 'logarithms' of these commuting matrices. The vectors of the F-system have a special role to play in the construction of the 3D adaptive Fibonacci grid; at every point of the 'zone plane' defining a particular ratio of the three components of orthogonal deformation to which the Fibonacci grid is subjected, six of the vectors collectively form the six generators of the appropriate 'hexad' of generalized lattice lines along which finite differencing is carried out. The six line-derivatives can then be combined to form the spatial gradient. The lattice hexads are precisely those defined by the algorithm of that name used at NCEP in the production of anisotropic covariances for meteorological data assimilation (Purser et al. 2003; Purser 2005). In the data assimilation context, hexads conform to a covering of the six-dimensional space of symmetric second moment 'aspect tensors' by non-overlapping 'tiles' which each form a cone of six-pointed simplex cross-section. Gaussian smoothing filters with the desired aspect tensor are reconstructed by sequentially smoothing, with one-dimensional

filters, along the six lines prescribed by the hexad and with smoothing strengths (as measured by second moments in grid-spacing units along each of the six lines) proportional to the six 'weights' that emerge as the projection of the aspect tensor into the given hexad basis. In the present context, the six hexad weights can be multiplicatively combined in threes and these triple products, or monotonic functions of them that fade smoothly to zero, used to weight the representation of the gradient associated with finite differencing along the corresponding three lattice lines. There are 20 ways to choose three lines from a hexad, but only 16 of these correspond to linearly independent directions (the hexad lines exactly correspond to the six diameters of a cuboctahedron and there are four planes that each contain three of these diameters; being linearly dependent, these triples must be disallowed). Thus, the 3×6 matrix by which the six line-derivatives are locally combined to form the gradient is implicitly built up from the 16 aforementioned contributions in a perfectly systematic and well-defined way.

The connection with the 'hexad algorithm' comes about because, for any valid deformation (i.e., one that is correctly aligned with the three eigenvectors of the $\boldsymbol{M}_\alpha$) the algorithm uniquely defines how an isotropic Gaussian is decomposed into line-smoothing operators. The appropriate hexad can be found for each point in the plane whose coordinates are proportional to the logarithms of the deformation components – the 'zone plane'. We may also contour, in this plane, the 'distance' (in the sense defined by Purser 2005) to the middle of the corresponding hexad. The middle, or centroid, of the hexad corresponds to a deformation of the lattice (not allowed by the rules for Fibonacci deformations) that would make the lattice one of the 'closest-packing' or 'face-centered cubic' arrangements, with the six opposing pairs of nearest neighbor directions corresponding to the hexad's line directions. Such a contouring is shown in Fig. 8 for a part of the zone plane and with the log-deformation coordinates arranged in the most symmetrical way. Note that, since we are not concerned with the magnitude of the determinant of the deformation (i.e., the absolute Jacobian) the standardized parameter space for such deformations reduces to two dimensions instead of three. The F numbers are also plotted in their natural positions, together with the vectors they form. The hexad boundaries are clearly seen as kinks in the centroid-distance contours. Each F-number vector corresponds to the particular lattice line it generates. A particular vector's lattice line achieves a dominance among the hexads which are active where that vector is plotted on the zone map. The particular vector, $[1, 0, 0]$, is singled out in Fig. 8 to show, by the slightly darker shaded and heavy-bordered region, the 24 hexads in which it participates. From a copy of this figure a mask can be made with the shaded region forming an aperture. Rotating the mask (same side up) 180° allows one to see which six F-vectors form the hexad of any given point in this zone-map.

If we standardize the map of deformation by normalizing according to the *trace* of each matrix rather than the *determinant* another natural mapping, the 'gnomonic' zone map, is found. In this case, the original zone plane is mapped to the interior of a triangle, which is most symmetrically represented as an equilateral triangle and, as shown in Fig. 9, the boundaries between the hexads now map to straight line segments. The contours of the hexad weights also form straight line segments in this projection.

In this mapping, it is possible to represent non-standard deformations where some of the deformation components are negative. In fact, if we were to take the unnormalized matrices of the quasi-Fibonacci systems as if they (rather than their squares) represented the relative aspect tensors, we would find that, in each of the systems F, F' and F'', the lattices of these

numbers separate into four interleaved half-resolution grids whose members generically map to the gnomonic projection in the following ways: If the triple-index vector is completely even (all three components divisible by two), then the mapping is to the *interior* of the equilateral triangular region; but if the lattice is one of the three other shifted half-resolution lattices, then mapping is to a region formed by the union of an opposing pair of sectors outside the triangle and having the same two 'produced' lines of this triangle as the region boundary (clearly, there are three such combined exterior regions). A straight line through this gnomonic projection plane maps back to the original zone plane as a three-asymptote 'tricorn', as shown for two such curves in Fig. 10. We see that such tricorns are all mutually congruent and identically oriented. This figure also deliberately shows how short segments of such tricorns serve as the hexad boundaries in the original zone map. The natural geometry for any gnomonic map is classical projective geometry (Coxeter 1987). For the plane, this geometry includes points at infinity in each of 180° of direction, and a single 'line at infinity' that connects them. We might inquire what curve this most isotropic 'line at infinity' corresponds to in the original zone plane. The answer is that it corresponds to the most symmetricaly-placed tricorn, centered on the origin. The matrices in the F-systems for which the traces of their squares vanish, always have their index points lying on this most symmetrical tricorn.

6. Algebraic identities related to asymptotic approximations

Another curious pattern emerges when we look at the cyclic sums of integer powers of the roots, R_α. Since these cyclically permute as the ordered eigenvalues of $\boldsymbol{M}_0$, $\boldsymbol{M}_1$ and $\boldsymbol{M}_2$, and from the trace identity, 4.13a, we find that:

$$\text{trace}(\boldsymbol{M}_0^p \boldsymbol{M}_2^q) \equiv \sum_{\alpha=0}^{2} R_\alpha^p R_{\alpha-1}^q = F''_{2p-q,-p+2q,-p-q}, \tag{6.1}$$

or,

$$\text{trace}(\boldsymbol{M}_0^p \boldsymbol{M}_1^q \boldsymbol{M}_2^r) \equiv \sum_{\alpha=0}^{2} R_\alpha^p R_{\alpha+1}^q R_{\alpha+2}^r = (-)^r F''_{2p-q-r,2r-p-q,2q-p-r}. \tag{6.2}$$

The dot-product identities can be used to derive from this expression various other (but more complicated) cyclic sum formulae for the F-numbers and F'-numbers. We may also use (6.1) to examine and explain the very obvious feature of the Figs. 5, 6 and 7 — namely the presence and orientations of directions 120° apart close to which the numerical magnitudes of the F-, F'- and F''-numbers are invariably much smaller than those of the numbers at corresponding distances from the origin along other radii. For example, take the quantity, $F''_{-19,14,5} = 9$, which is formed by (6.1) from the sum of three terms:

$$\begin{aligned} F''_{-19,14,5} = 9 \quad &= \quad R_0^{-8} R_2^3 + R_2^{-8} R_1^3 + R_1^{-8} R_0^3 \\ &\approx \quad 0.000263 - 57.32449 + 66.32423. \end{aligned} \tag{6.3}$$

Here we have a negligible first term and the other two terms approximately opposite and equal. For exact equality of the second two terms we would require that the two exponents in (6.1) be

in the ratio:

$$\begin{aligned}\frac{q}{p} &= \frac{\log|\frac{R_1}{R_2}|}{\log|\frac{R_1}{R_0}|}, \\ &= \frac{\log R_0 + 2\log R_2}{\log R_2 + 2\log R_0}, \\ &\approx -0.357308. \end{aligned} \tag{6.4}$$

In the opposite direction in the F''-numbers we find that the three terms that sum to form $F''_{19,-14,-5} = 3802$ are the reciprocals of what we found before, that is, the first term now dominates:

$$\begin{aligned} F''_{19,-14,-5} = 3802 &= R_0^8 R_2^{-3} + R_2^8 R_1^{-3} + R_1^8 R_0^{-3} \\ &\approx 3802.0023 - 0.017 + 0.015. \end{aligned} \tag{6.5}$$

Moreover, this first-term dominance tends to hold throughout the interior of this broad sector of the relatively large F''-numbers, and, by virtue of the dot-product relations, therefore within the corresponding sectors of the F- and F'-numbers. This gives rise to several useful asymptotic results that hold within this 'positive sector', such as:

$$R_0 \approx +\frac{F_{i+2,j-1,k-1}}{F_{i,j,k}}, \tag{6.6a}$$

$$R_1 \approx -\frac{F_{i-1,j-1,k+2}}{F_{i,j,k}}, \tag{6.6b}$$

$$R_2 \approx +\frac{F_{i-1,j+2,k-1}}{F_{i,j,k}}, \tag{6.6c}$$

which are exactly analogous to the way ratios of the consecutive large true Fibonacci numbers relate to the 'golden ratio'. These identities tend to be particularly accurate at positions in the number arrays close to the positive ray that corresponds to exponents p and q in the ratio given by (6.4), or equivalently, with indices, (i, j, k), close to the ratio:

$$\begin{aligned} i:j:k &= \log|R_0| : \log|R_2| : \log|R_1| \\ &\approx (0.809587) : (-0.588862) : (-0.220724). \end{aligned} \tag{6.7}$$

The angle, β, by which the figures 5–7 must be rotated to make the asymptotically 'relatively small' numbers in the left of these diagrams line up horizontally, as they do in Figs. 8 and 10, can be shown from (6.7) to be such that:

$$\begin{aligned} \tan(\beta) &= \frac{\log|R_1| - \log|R_2|}{\sqrt{3}\log|R_0|} \\ &\approx \tan(14.71^\circ). \end{aligned} \tag{6.8}$$

Approximations to the components of the normalized eigenvectors are given within what we are calling the 'positive sector' by:

$$v_0 \approx \frac{F_{i+1,j,k-1}}{F'_{i,j,k}}, \tag{6.9a}$$

$$v_1 \approx \frac{F_{i,j-1,k+1}}{F'_{i,j,k}}; \tag{6.9b}$$

$$v_2 \approx -\frac{F_{i-1,j+1,k}}{F'_{i,j,k}}, \tag{6.9c}$$

The approximations (6.9a)–(6.9c) located close to where indices approximate the ratio, (6.7), are particularly useful in fixing the single- or double-periodicity conditions for the 3D Fibonacci grids whose skeleton grids have either one or two periodic coordinates respectively. Again, the situation is analogous to the role of the genuine Fibonacci numbers in determining the numbers of spirals in the 2D Fibonacci grid.

The quasi-Fibonacci numbers also exhibit the 'duplication formulae':

$$F_{2\boldsymbol{i}} + (-)^k 2F_{-\boldsymbol{i}} = (F'_{\boldsymbol{i}})^2, \tag{6.10a}$$

$$F'_{2\boldsymbol{i}} + (-)^k 2F'_{-\boldsymbol{i}} = 7(F_{\boldsymbol{i}})^2, \tag{6.10b}$$

$$F''_{2\boldsymbol{i}} + (-)^k 2F''_{-\boldsymbol{i}} = (F''_{\boldsymbol{i}})^2. \tag{6.10c}$$

where $\boldsymbol{i}$ denotes the composite index, $\boldsymbol{i} = (i, j, k)$. There are analogous formulae for the true Fibonacci and Lucas numbers. Note that the ubiquitous occurrence of 'fives' in the theory of classical Fibonacci and Lucas numbers is replaced by the 'sevens' we find throughout the algebraic development of the quasi-Fibonacci numbers.

7. Generalization at higher dimensions

As the appendix makes clear, there is a clearly defined pattern by which it is possible to generalized the two-dimensional geometrical grid construction associated with the classical Fibonacci numbers to exactly analogous grid constructions in some higher dimensions, together with infinite arrays, now themselves multi-dimensional of the correspondingly analogous 'quasi-Fibonacci' natural numbers. Apart from the three dimensional case we have dealt with in this article, the only other dimensionality that could be of conceivable practical use in geophysical modeling or data assimilation is the four-dimensional case which, owing to the fact that $2n + 1$ is not a prime number in $n = 4$ dimensions, cannot be included in the family of generalizations analyzed in the appendix.

Nevertheless, it is possible to search for alternative constructions in four dimensions, each characterized by a sufficiently complete set of mutually-commuting order-four integer-component matrices. The merit of each example found could be measured objectively by the magnitude of the largest radius of the voronoi cell of the associated deformation-space lattice that picks out the 'hypercubic' locations of the deformed Fibonacci-type grid; this measures the maximum possible deformation-distance from perfectly cubic that the Fibonacci grids associated with such a system can ever suffer. Therefore, a small Voronoi radius is an indicator of a good generalized Fibonacci grid system. Unfortunately, the 'best' four-dimensional Fibonacci grid generalization by this measure, having a Voronoi cell largest radius of about 0.94 dimensionless units of deformation, possesses very little symmetry in its deformation-space lattice. If we are willing to accept a somewhat larger magnitude of maximum departure from the perfectly (hyper-)cubic Fibonacci lattice, having a Voronoi radius of about 1.2 units of deformation, then

a much more symmetrical lattice of commuting unimodular integer-component matrices can be found.

One basis for this recommended system is provided by the three matrices:

$$\boldsymbol{N}_0 = \begin{bmatrix} 1, & 1, & 0, & 0 \\ 1, & 0, & 0, & 0 \\ 0, & 0, & 1, & 1, \\ 0, & 0, & 1, & 0 \end{bmatrix}, \tag{7.1a}$$

$$\boldsymbol{N}_1 = \begin{bmatrix} 1, & -1, & 1, & 0 \\ -1, & 2, & 0, & 1 \\ 1, & 0, & 0, & 0 \\ 0, & 1, & 0, & 0 \end{bmatrix}, \tag{7.1b}$$

$$\boldsymbol{N}_2 = \begin{bmatrix} 1, & 0, & -1, & -1 \\ 0, & 1, & -1, & 0 \\ -1, & -1, & 1, & 1 \\ -1, & 0, & 1, & 0 \end{bmatrix}. \tag{7.1c}$$

Powers of the first basis, $\boldsymbol{N}_0$, are simply block-diagonal replications of the powers of the the classical two-dimension Fibonacci matrix. The degeneracy of the eigen-structure is only resolved when the other members, $\boldsymbol{N}_1$ and $\boldsymbol{N}_2$, of the basis are included. We find that any product of integer powers of these unimodular matrices or their inverses produces another matrix, say $\boldsymbol{A}$, having as its most obvious additional symmetry, the property:

$$A_{1,4} = A_{2,3}. \tag{7.2}$$

Recall that

$$\phi = \frac{1+\sqrt{5}}{2},$$

and define four coefficients:

$$a^{\pm} = 3 \pm \sqrt{5}, \tag{7.3a}$$

$$b^{\pm} = \sqrt{6(5 \pm \sqrt{5})}, \tag{7.3b}$$

and from these,

$$\nu_1 = \frac{a^- - b^-}{4} \approx -0.827090915285, \tag{7.4a}$$

$$\nu_2 = \frac{a^+ - b^+}{4} \approx -0.338261212718, \tag{7.4b}$$

$$\nu_3 = -\nu_1^{-1} = \frac{a^- + b^-}{4} \approx 1.20905692654, \tag{7.4c}$$

$$\nu_4 = -\nu_2^{-1} = \frac{a^+ + b^+}{4} \approx 2.95629520147. \tag{7.4d}$$

Then the eigenvalues of $\boldsymbol{N}_{(\alpha)}$ are given by the elements of the diagonal matrices:

$$\begin{aligned} \boldsymbol{V}^T\boldsymbol{N}_0\boldsymbol{V} &= \text{diag}\{\phi, -\phi^{-1}, \phi, -\phi^{-1}\}, && \text{(7.5a)} \\ \boldsymbol{V}^T\boldsymbol{N}_1\boldsymbol{V} &= \text{diag}\{\nu_1, \nu_2, \nu_3, \nu_4\}, && \text{(7.5b)} \\ \boldsymbol{V}^T\boldsymbol{N}_2\boldsymbol{V} &= \text{diag}\{\nu_4, \nu_1, \nu_2, \nu_3\}, && \text{(7.5c)} \end{aligned}$$

with the eigenvector matrix being of the form,

$$\boldsymbol{V} = \begin{bmatrix} \phi g, & h, & \phi\nu_3 g, & \nu_4 h \\ g, & -\phi h, & \nu_3 g, & -\phi\nu_4 h \\ -\phi\nu_3 g, & -\nu_4 h, & \phi g, & h \\ -\nu_3 g, & \phi\nu_4 h, & g, & -\phi h \end{bmatrix}, \qquad (7.6)$$

and with g and h chosen to ensure these eigenvectors are properly normalized:

$$\begin{aligned} g &= [(1+\nu_3^2)(1+\phi^2)]^{-1/2} \approx 0.3350700804456, && \text{(7.7a)} \\ h &= [(1+\nu_4^2)(1+\phi^2)]^{-1/2} \approx 0.1684578700610. && \text{(7.7b)} \end{aligned}$$

$\boldsymbol{N}_1$ and $\boldsymbol{N}_2$ are similar, sharing exactly the same eigenvalues. In all the matrices, eigenvalues occur in negative-reciprocal pairs. Another symmetry relates to the deformation-metrical properties of these three basic matrices: in deformation-space they are all mutually-orthogonal with respect to the deformation metric. Therefore, the lattice of the deformation-space points that mark the locus of each instance of a generalized Fibonacci grid configuration that is precisely cubic, is itself an orthogonal lattice possessing equal spacing in the $\boldsymbol{N}_1$ and $\boldsymbol{N}_2$ directions (the spacing in the $\boldsymbol{N}_0$ direction being smaller).

With such a high degree of symmetry it is no surprise that the associated 'quasi-Fibonacci' numbers that encode the possible matrix products fall into a tidy lattice arrangement. The symmetry, (7.2), leaves nine distinct components of the generic product, $\boldsymbol{A}$, of arbitrary integer powers of the $\boldsymbol{N}_{(\alpha)}$. These can be arranged in a 3×3 array according to the scheme:

$$\boldsymbol{A} \equiv \begin{Bmatrix} A_{2,2}, & A_{1,2}, & A_{1,1} \\ A_{2,4}, & A_{1,4}, & A_{1,3} \\ A_{4,4}, & A_{3,4}, & A_{3,3}, \end{Bmatrix} \qquad (7.8)$$

and this pattern then efficiently encodes all possible product matrices formed of the three basis matrices when the quasi-Fibonacci numbers of this system are placed at the three-dimensional deformation-lattice points according to the scheme whose central portion is depicted in Fig. 11. Here the exponents of $\boldsymbol{N}_0$, $\boldsymbol{N}_1$, $\boldsymbol{N}_2$ are denotes X, Y and Z respectively. Each matrix $\boldsymbol{A}$ is encoded by the 3×3 sub-array arrangement on the constant Z layer centered at the corresponding lattice location. Thus, the identity matrix at the origin is encoded by the central square of numbers of level $Z = 0$:

$$\boldsymbol{I} \equiv \begin{Bmatrix} 1, & 0, & 1 \\ 0, & 0, & 0 \\ 1, & 0, & 1 \end{Bmatrix}. \qquad (7.9)$$

The generalized Fibonacci grids constructed according to this scheme (or one of the viable less symmerical alternatives that can be found) would, in principle, allow a gradual and coordinated enhancement of the resolution of both space and time together. For numerical modeling applications this implies the acceptance of the new challenge of designing fully asynchronous time integration schemes (no two space-time grid points actually occur at the same time!) For applications in data assimilation this curious feature of the grid is probably much less of a problem since most of the numerical operations involved do not presuppose synchroneity.

8. Discussion and Conclusion

We have introduced a new class of computational lattices for applications in atmospheric data assimilation and possibly for numerical weather prediction. The essential characteristic of these 'generalized Fibonacci grids' is their ability to acquire high resolution in several independent locations while preserving the overall unity of the grid. In any given region, the grid appears perfectly regular (though curvilinear, of course), so any standard numerical line-operations, such as finite differencing, integration, filtering or interpolation, should remain quite straightforward to apply. In the case of the special version of the Fibonacci grid with uniform resolution over the sphere, Swinbank and Purser (1999, 2006) demonstrated that the unusual configuration of this grid is no impediment to achieving successful integrations of a prediction model.

In two dimensions, the number of degrees of freedom available in the construction of the guiding 'skeleton grid', which must remain approximately orthogonal everywhere, is exactly the number needed to allow regions of enhanced resolution to be defined more or less arbitrarily. There is not complete freedom, however, because the grid over the surface of the sphere must still satisfy certain global topological constraints in order to remain free of singularities. In the three dimensional generalization of the adaptive qusi-Fibonacci grid system, the number of orthogonality constraints imposed on the construction of the skeleton grid restrict how the associated Fibonacci grid can be adapted in a fully three-dimensional way. Crudely speaking, the three independent constraints of orthogonality of the three-dimensional skeleton grid leave no spare degrees of freedom left over to let this grid's Jacobian faithfully follow any arbitrarily prescribed geographical distribution. The six constraints of orthogonality in the four-dimensional case are clearly even more restricting. Nevertheless, in these higher dimensions, as long as we are prepared to adjust the effective metric we are using in our definition of 'orthogonality', we still have the ability to allow the grid to concentrate in regions where a higher resolution is needed.

The methods by which the orthogonal grid can be generated in response to the user's preference for enhanced resolution will be the topic of a future note. The best approach seems to be a variational one, Although there is a literature for such methods (for example, Thompson et al. 1985) the preservation of the (approximate) constraint of orthogonality is a delicate problem that requires a special treatment.

At the present time it would appear that using these grids in data assimilation will be less problematic than using them for the numerical integration of the dynamical equations. There is very little practical experience in using a fully general curvilinear grid for numerical weather prediction. In some very specialized theoretical computations, such as in semi-geostrophic

theory, it is customary to adopt a smoothly distorted grid transformation which, in three dimensions, leaves the 'vertical' directions of the computational lattice canted with respect to the true vertical, but this is an unnatural-looking grid for the modelling of hydrostatic equations of motion where the equations are strongly coupled in the strictly vertical direction. However, as the adoption of nonhydrostatic equations becomes more and more widespread, the need for the computational lattice to be so strictly constrained disappears. Even such 'vertical' processes as the fall of precipitation or the penetration through the atmosphere of incoming radiation are not strictly confined to vertical directions in reality and, presumably, could be equally well dealt with in some more general coordinate system such as the quasi-Fibonacci grid proposed here. The real difficulty will be designing numerical integration methods for the hydrodynamic equations on unstaggered curvilinear grids which remain sufficiently stable through large changes in spatial resolution while being sufficiently efficient computationally to be contenders for future numerical weather prediction systems for operations.

While we have introduced the mathematical framework by which a four-dimensional grid of the generalized Fibonacci type can, in principle, be constructed, we are even less able to answer the question, for this dimensionality, of whether such a grid could supply a viable framework for a prediction model. Compounding the challenges we have mentioned for the three-dimensional case, it would now be necessary to adopt stable numerical schemes that are also able to cope with the complete lack of any temporal synchroneity between any pairs of the space-time lattice points. Presumably, similar challenges have been faced and successfully met in the realm of relativistic astrophysical models for which, again, the concept of synchroneity is absent (though for the reason of physical necessity rather than of numerical choice). The advantage of a full four-dimensional adaptive grid framework is that, where the spatial resolution is made finer, the temporal resolution automatically becomes finer in the appropropriate proportion. This could be a helpful factor in maintaining computational stability and in maximimizing the overall efficiency (by not wasting excessively short time steps in the coarser-resolved regions where they are certainly not needed). As in the three-dimensional case, the path to using these grids for data assimilation seems a lot more straight-forward and most of the necessary numerical tools, in the form of adaptive covariance generators and interpolation procedures, are already available and could therefore be easily adopted.

Acknowledgments

The original Fibonacci grid was developed in close collaboration with Dr. Richard Swinbank of the Met. Office; without his initial impetus and perseverance in demonstating the practical feasibilty of the original homogeneous-resolution Fibonacci grid system, the generalizing extensions described here could not have been conceived. The author also benefitted from stimulating discussions with Dr. David Parrish, NOAA/NCEP/EMC, and Dr. W. Carlisle Thacker of NOAA/AOML.

Appendix A

Eigen-structure of n-dimensional quasi-Fibonacci matrices

Define $\boldsymbol{M}^{(n)}$ to be the n-dimensional Fibonacci matrix with components,

$$M^{(n)}_{i,j} = \begin{cases} 1 & : \quad i+j \leq n+1 \\ 0 & : \quad i+j > n+1 \end{cases} . \tag{A.1}$$

Then the inverse has components:

$$\left(\boldsymbol{M}^{(n)}\right)^{-1}_{i,j} = \begin{cases} 1 & : \quad i+j = n+1 \\ -1 & : \quad i+j = n+2 \\ 0 & : \quad \text{otherwise} \end{cases} , \tag{A.2}$$

and the square of this matrix has components:

$$\left(\boldsymbol{M}^{(n)}\right)^{-2}_{i,j} = \begin{cases} 1 & : \quad i=j=1 \\ 2 & : \quad i=j>1 \\ -1 & : \quad |i-j|=1 \\ 0 & : \quad \text{otherwise} \end{cases} . \tag{A.3}$$

Thus, $(\boldsymbol{M}^{(n)})^{-2}$ is the explicit matrix representation of the simplest possible finite-difference approximation to the one-dimensional negative-Laplacian on a unit grid, $i = 1, \ldots, n$, where a Neumann boundary condition (zero derivative) is implicitly assumed at $i = \frac{1}{2}$, while a Dirichlet boundary condition (zero value) is implicitly assumed at $i = n+1$. Eigenvectors of $(\boldsymbol{M}^{(n)})^{-1}$ (and hence of $\boldsymbol{M}^{(n)}$ itself) must therefore be those that correspond to 'quarter-period' discrete Fourier transforms in which the wavelengths of the sinusoidal eigenvectors conforming to the boundary conditions are odd-number multiples of the fundamental wavelength. The unnormalized eigenvector matrix $\boldsymbol{V}$ can be assumed symmetric with components,

$$V_{i,j} = \cos\left[\frac{(2i-1)(2j+1)\pi}{4n+2}\right], \tag{A.4}$$

where the eigenvalue index j runs from 0 to $n-1$. The corresponding eigenvalues, R^{-2}, of $(\boldsymbol{M}^{(n)})^{-2}$ are easily found to obey,

$$R_j^{-2} = 4\sin^2\left(\frac{(2j+1)\pi}{4n+2}\right), \tag{A.5}$$

and, after a careful verification of the appropriate signs, those of $\boldsymbol{M}^{(n)}$ itself are found to be:

$$R_j = \frac{(-)^j}{2\sin\left[(2j+1)\pi/(4n+2)\right]}. \tag{A.6}$$

For the case, $n = 2$, we recover the familiar 'golden ratio' numbers:

$$R_0 = \frac{1}{2\sin(\pi/10)} = \phi \approx 1.618, \tag{A.7}$$

$$R_1 = \frac{-1}{2\sin(3\pi/10)} = -1/\phi \approx -0.618. \tag{A.8}$$

For the case $n = 3$ that is the main focus of this paper,

$$R_0 = \frac{1}{2\sin(\pi/14)} \approx 2.247, \tag{A.9}$$

$$R_1 = \frac{-1}{2\sin(3\pi/14)} \approx -0.802, \tag{A.10}$$

$$R_2 = \frac{1}{2\sin(5\pi/14)} \approx 0.555. \tag{A.11}$$

From the symmetries of the cosine function in (A.4) and the properties of primes then, provided $(2n+1)$ is a prime number, we find that: (i) the absolute magnitudes of the components of an eigenvector are n distinct numbers; and (ii) the absolute magnitudes of the components of $\boldsymbol{V}$ in each eigenvector are all permutations of one another such that, from the first property, each magnitude appears precisely once in each row and column; (iii) the columns of $\boldsymbol{V}$ can be re-ordered so in a cycle of period n such that a set of n signed-permutation matrices (each having a single '1' or a '-1' in each row or column, otherwise of zeroes) advances the cycle without changing the relative order, and therefore forms a cyclic group of order n. These symmetries ensures that, sharing these same eigenvectors $\boldsymbol{V}$, there exist $(n-1)$ other matrices that are equivalent to $\boldsymbol{M}^{(n)}$ via similarity transformations that involve only signed row and column permutations of $\boldsymbol{M}^{(n)}$. To see this, note that each one of the signed permutations $\boldsymbol{G}$ acting on the left of $\boldsymbol{V}$ permutes its rows, and acting on the right of $\boldsymbol{V}$ performs the inverse permutation on $\boldsymbol{V}$'s columns, but, owing to the special structural relationship beween $\boldsymbol{G}$ and $\boldsymbol{V}$, the combination leaves the product unchanged:

$$\boldsymbol{GVG} = \boldsymbol{V}. \tag{A.12}$$

Thus,

$$(\boldsymbol{GMG}^T)(\boldsymbol{GVG}) = (\boldsymbol{GVG})(\boldsymbol{G}^T\boldsymbol{RG}) \tag{A.13}$$

shows that the eigenvalues are shuffled by the inverse similarity transformation to that of $\boldsymbol{M}$.

References

Conway, J. H., and R. K. Guy	1996	*The Book of Numbers.* Springer-Verlag, New York.
Coxeter, H. S. M.	1987	*Projective Geometry, 2nd Edition* Springer, New York. 162 pp.
Franco, B. J. O.	1993	Third-order Fibonacci sequences associated to a heptagonal quasiperiodic tiling of the plane. *Phys. Lett. A.,* **178,** 119–122.
Hannay, J. H., and J. F. Nye	2004	Fibonacci numerical integration on a sphere. *J. Phys. A: Math. Gen.,* **37,** 11591–11601.
Preparata, F. R., and M. I. Shamos	1985	*Computational Geometry: An Introduction.* Springer-Verlag, New York.
Purser, R. J.	2005	A geometrical approach to the synthesis of smooth anisotropic covariance operators for data assimilation. NOAA/NCEP Office Note 447, 60 pp.

Purser, R. J., W.-S. Wu, D. F. Parrish, and N. M. Roberts	2003	Numerical aspects of the application of recursive filters to variational statistical analysis. Part II: Spatially inhomogeneous and anisotropic general covariances. *Mon. Wea. Rev.,* **131,** 1536–1548.
Steinbach, P.	1997	Golden fields: a case for the heptagon. *Math. Magazine,* **70,** 22–31.
Swinbank, R., and R. J. Purser	1999	Fibonacci grids. *(Preprint) AMS 13th Conference on Numerical Weather Prediction,* Denver, CO. 77–78.
Swinbank, R., and R. J. Purser	2006	Fibonacci grids; A novel approach to atmospheroc modeling. *Quart. J. Royal Meteor. Soc.,* **132,** 1769–1793.
Terauchi, H., K. Kamigaki, T. Okutani, Y. Nishihata, H. Kasatani, H. Kasano, K. Sakaue, H. Kato and N. Sano.	1990	Synchrotron X-ray diffraction of third-order Fibonacci lattices. *J. Phys. Soc. Japan,* **59,** 405–407.
Thompson, J. F., Z. U. A. Warsi, C. W. Mastin	1985	*Numerical Grid Generation: Foundations and Applications.* North-Holland, New York.
Wituła, R., D. Słota, and A. Warzynski	2006	Quasi-Fibonacci numbers of the seventh order. *J. of Integer Sequences,* **9,** article 06.4.3, 1–28.

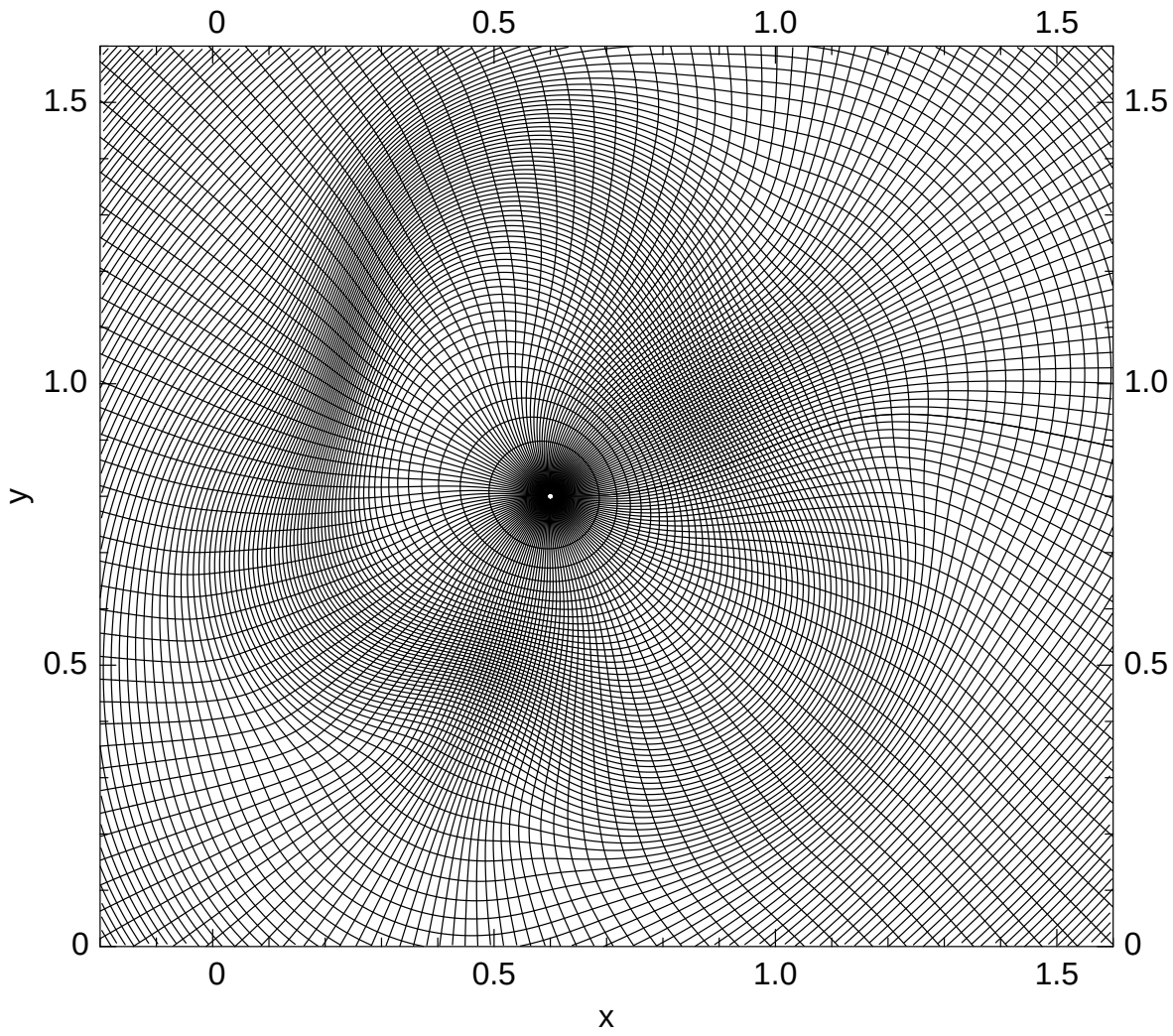

Figure 1. A two-dimensional polar skeleton grid constructed to be almost orthogonal and to enhance the areal resolution of the curvilinear grid cells in three specified regions.

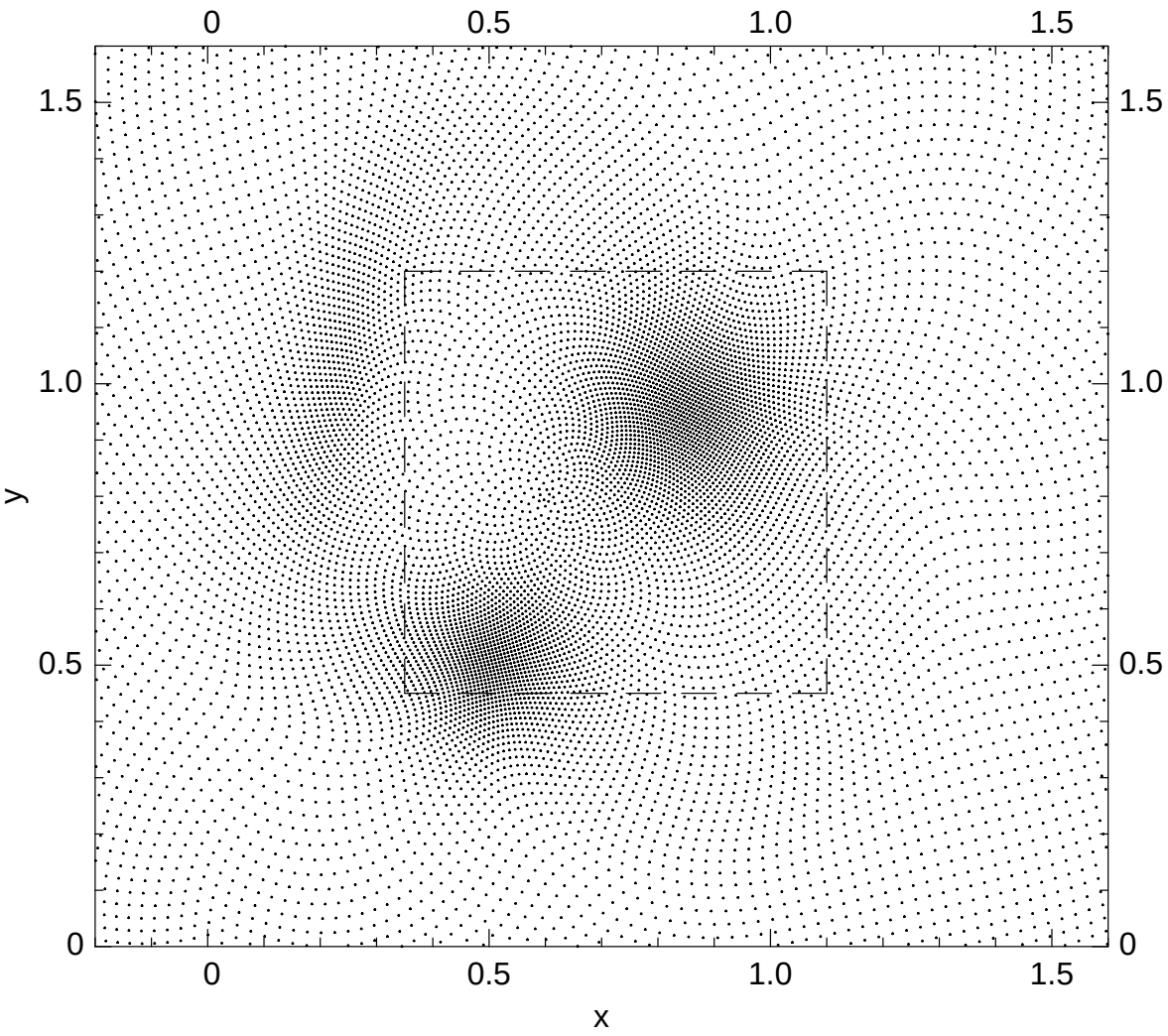

Figure 2. The generalized Fibonacci grid built upon the framework supplied by the skeleton grid of Fig. 1. The grid is locally never too far from appearing approximately isotropic in the sense that the distances to nearest neighbors remain consistent all around any chosen grid point. The subdomain marked out by the square is shown enlarged in Fig. 3

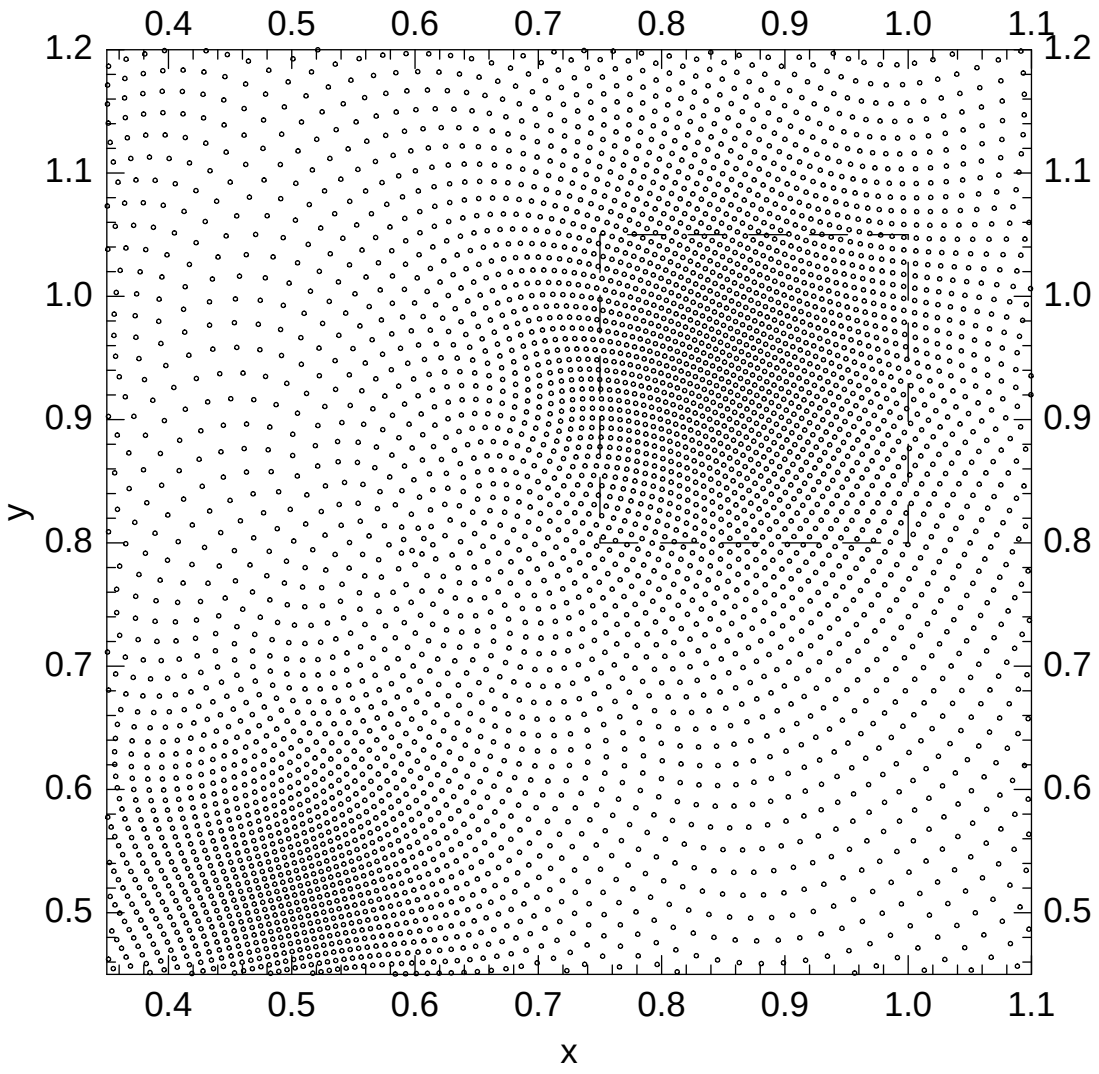

Figure 3. An expanded view of the subdomain indicated in the two-dimensional generalized Fibonacci grid of Fig. 2. The subdomain marked out by the square in the present figure is shown further enlarged in Fig. 4

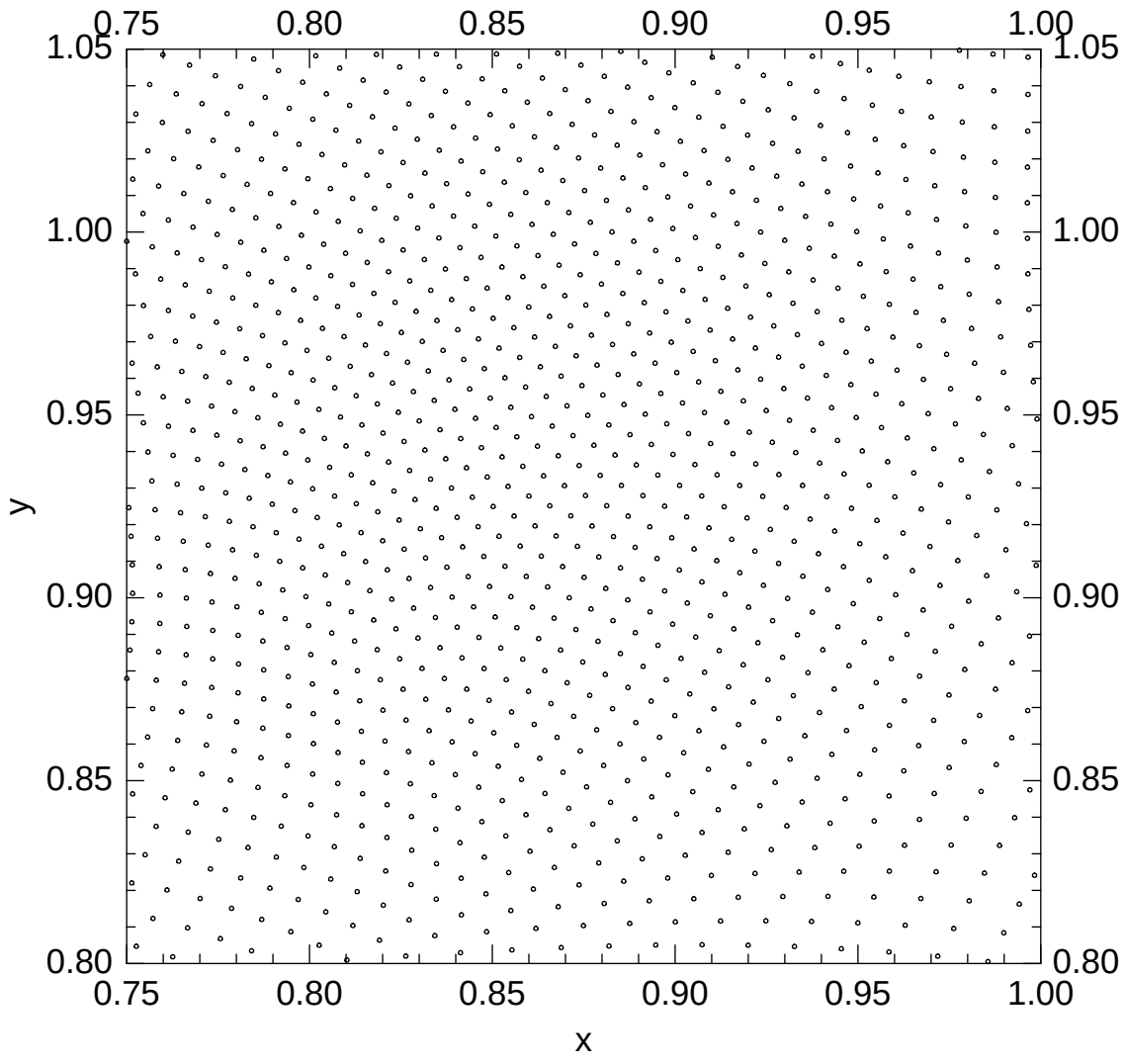

Figure 4. A further expanded view of the subdomain indicated in the two-dimensional generalized Fibonacci grid of Figs. 2 and 3, showing that, locally, the Fibonacci grid constructed upon the framework supplied by the skeleton grid of Fig. 1 appears locally to be perfectly smooth, and therefore suitable for numerical model integration or data assimilation.

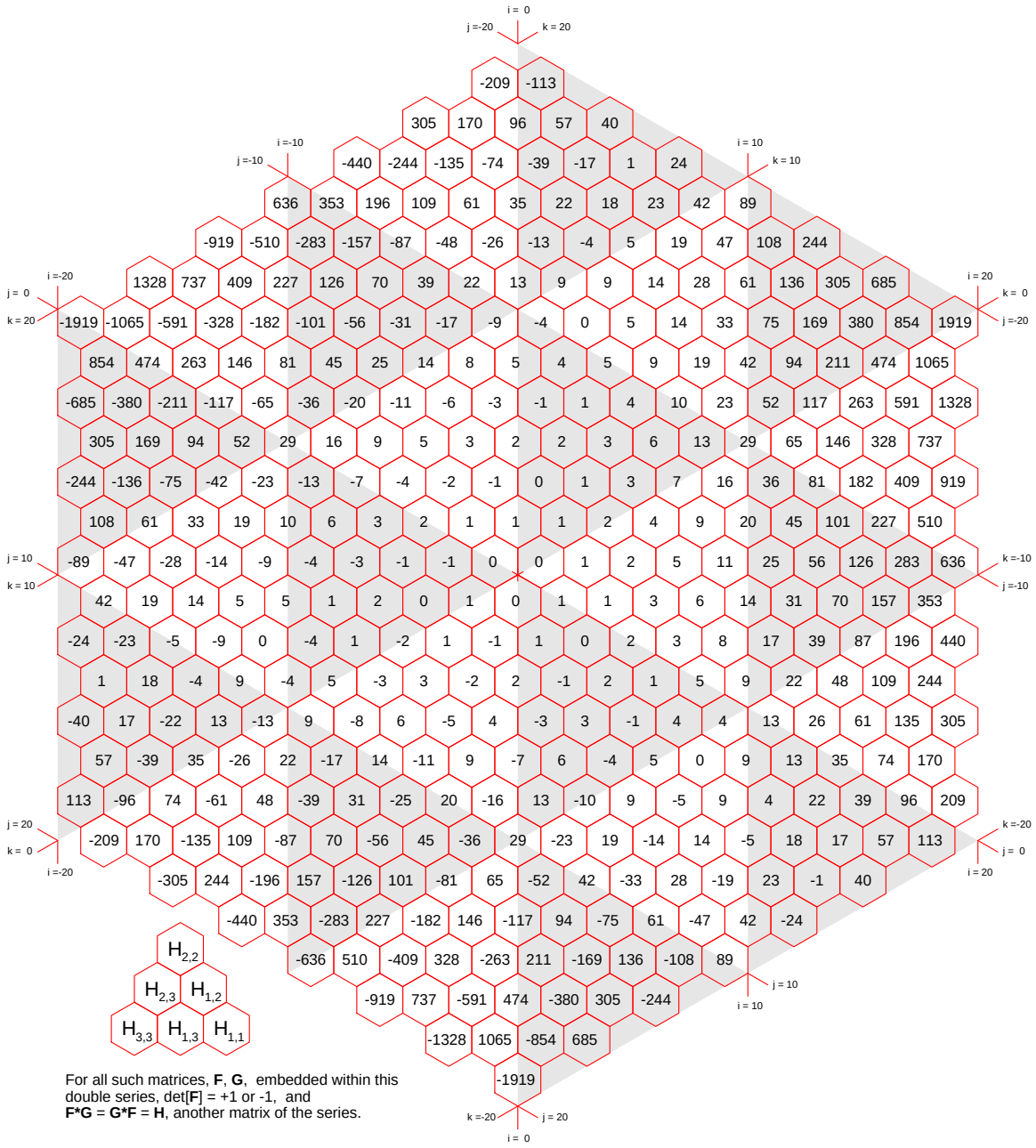

Figure 5. F-numbers. When indexed, (i, j, k), the index, i increases to the right (compass direction 90°), while j and k increase in the directions 210° and 330° respectively. The inset shows the configuration of a generic matrix encoded within these numbers, the index point of the matrix being the central point of this 3-high 'cannonball stack'. A corresponding 2-high stack defines a 3-vector hidden within this table of numbers.

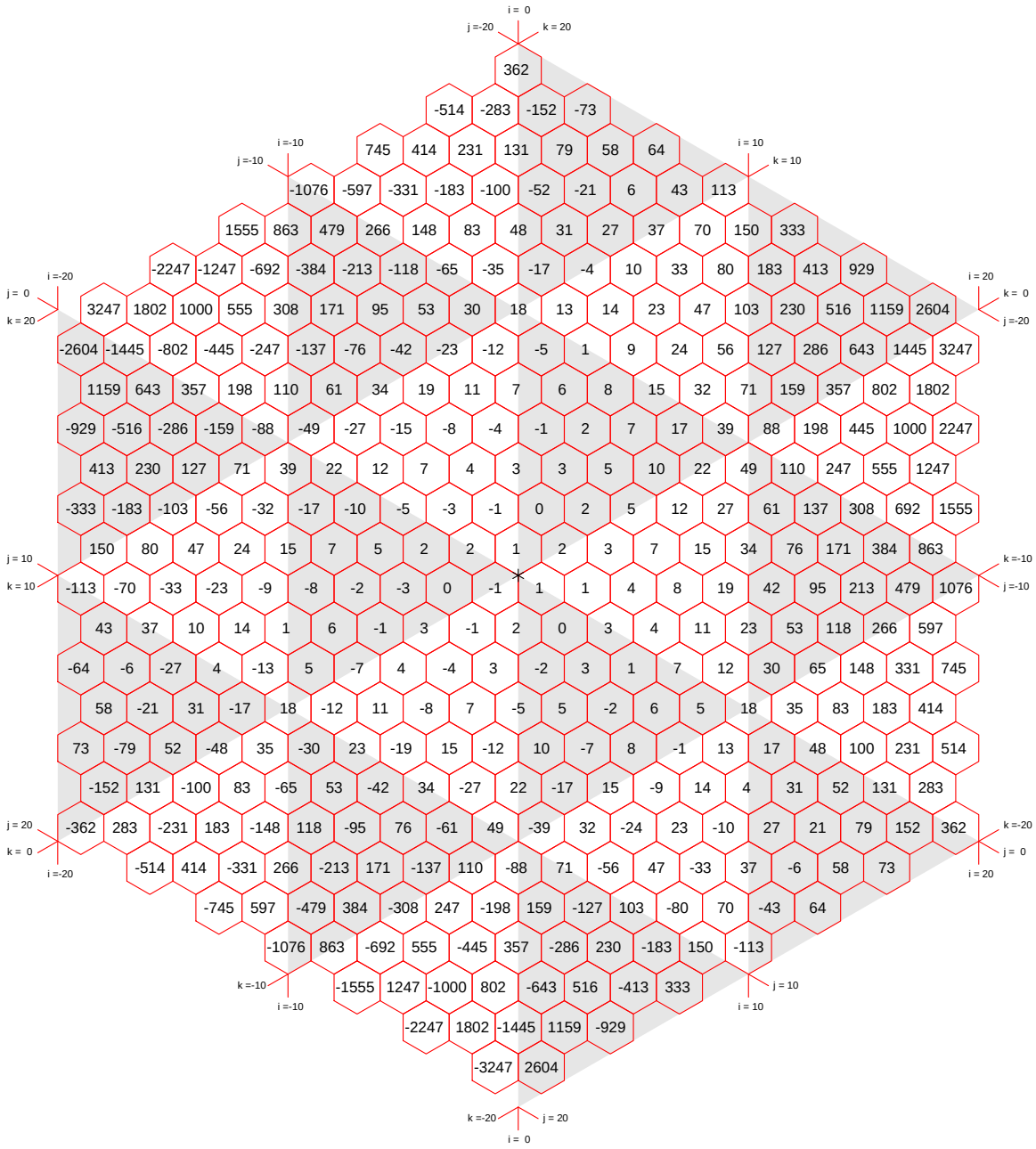

Figure 6. F'-numbers

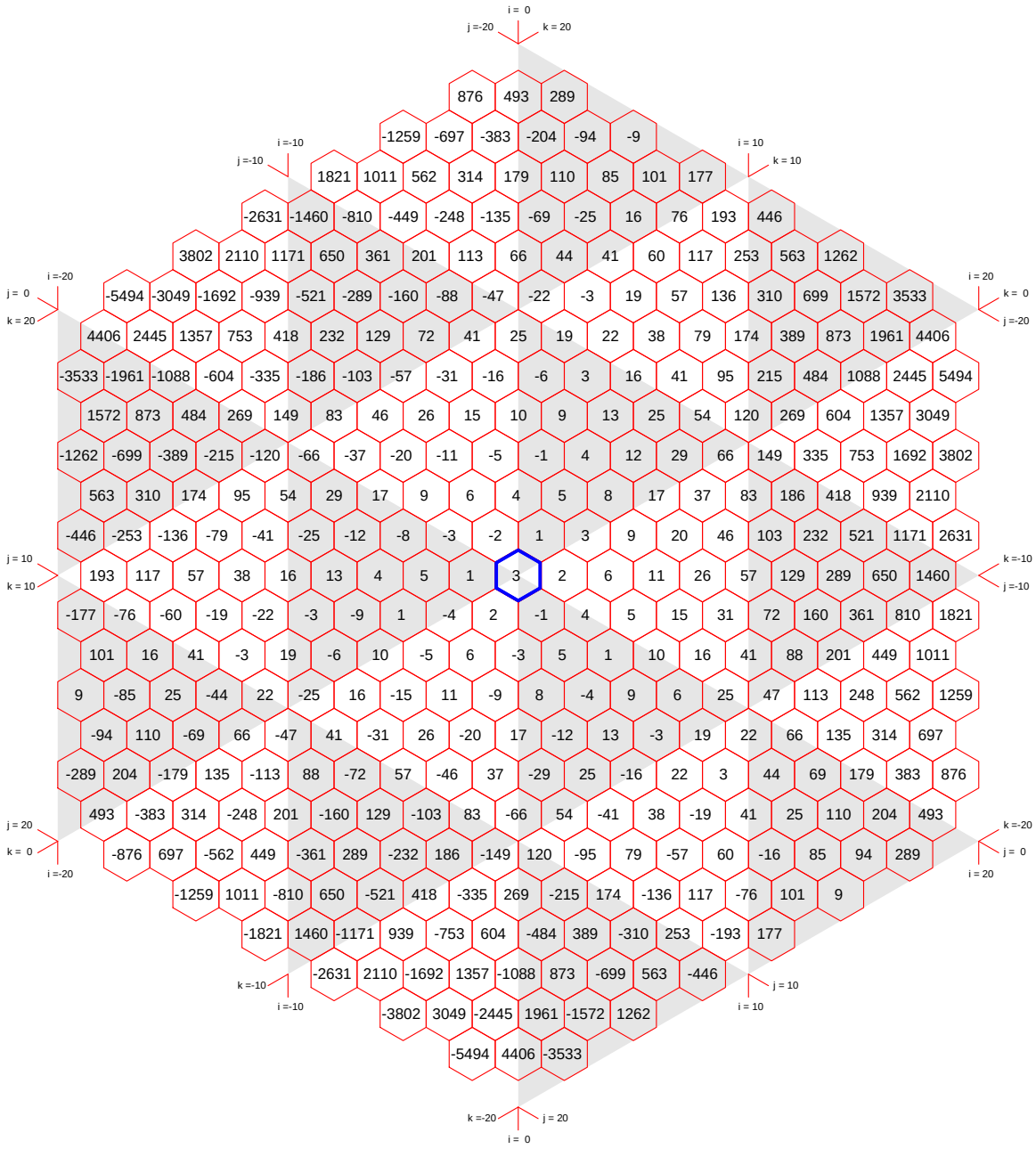

Figure 7. F''-numbers

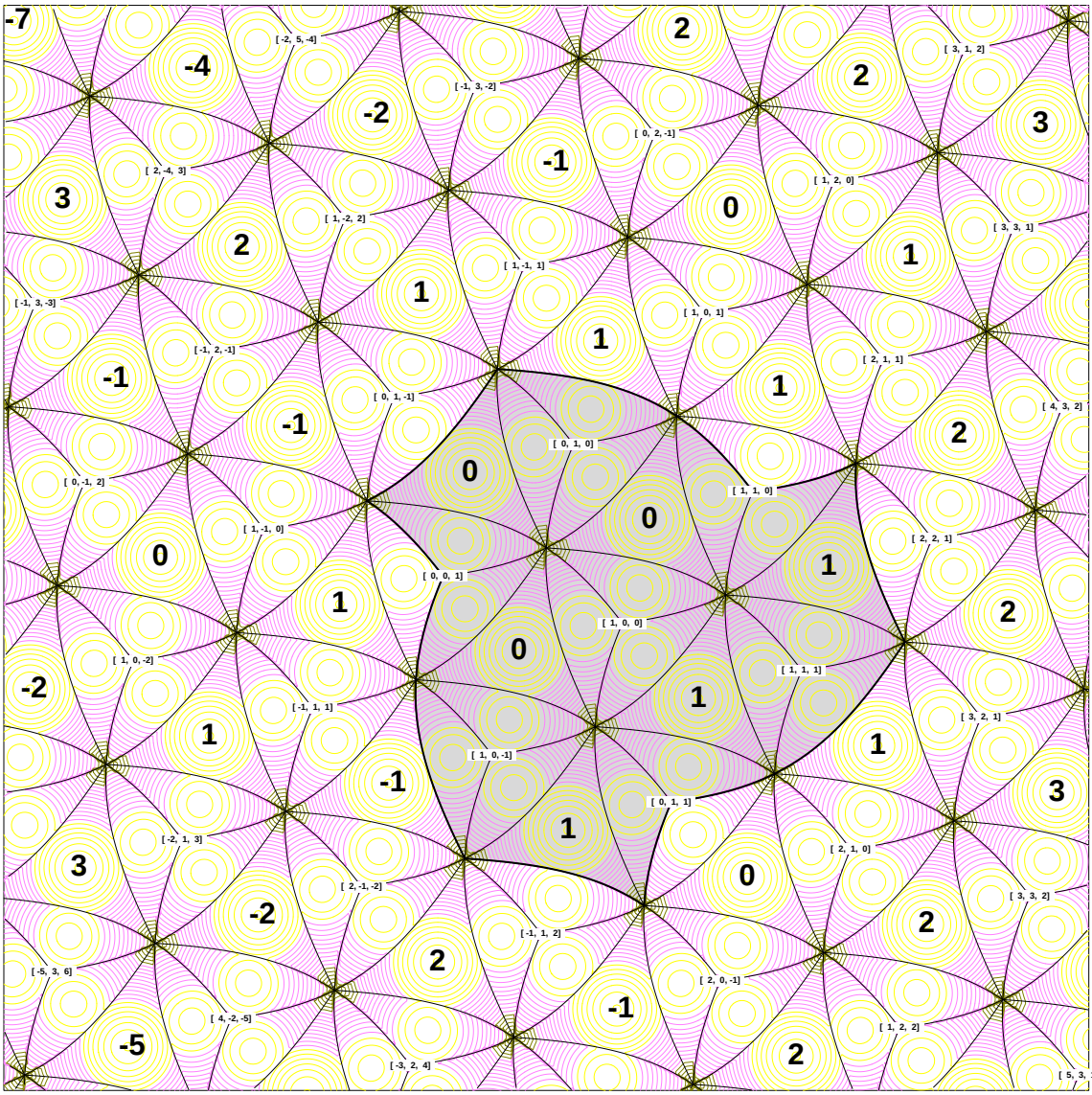

Figure 8. A part of the 'zone map' for zones of reconnection of the adaptive Fibonacci grid in three dimensions, together with F-numbers and associated vectors. The contours depict 'distance' of the appropriate hexad configuration, for each point in the zone map, to the centroid of that hexad, yellow contours being the smallest distances and black being the largest. A hexad is a natural lattice configuration of six families of line connections, and the centroid of the hexad corresponds to the case where these connections link nearest neighbors in a 'closest packing' or 'face centered cubic' arrangement. The points where nine hexad regions meet correspond to deformation parameters that happen to make the lattice cubic.

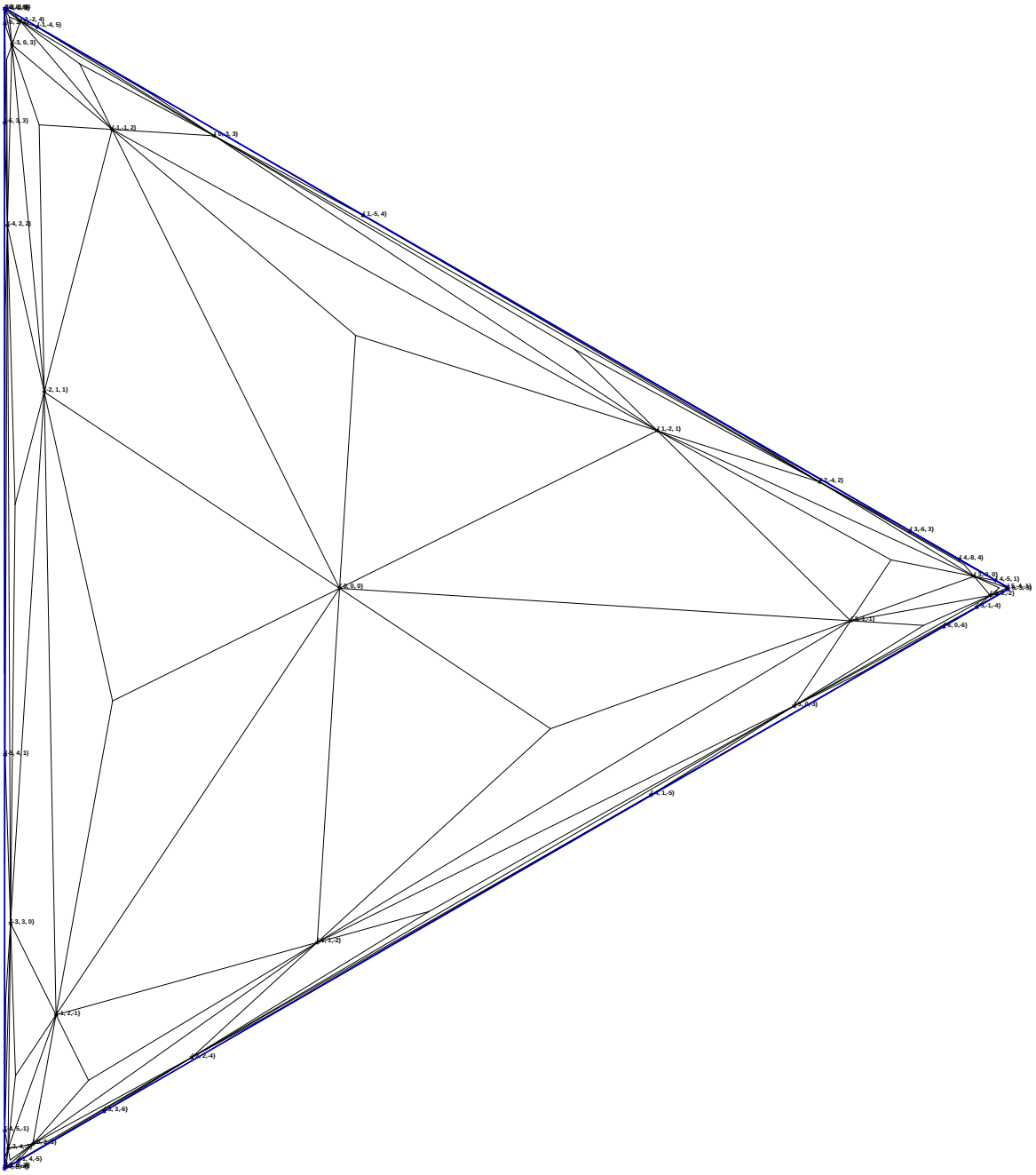

Figure 9. Gnomonic zone map whose projection center is aligned with the origin of Fig. 8

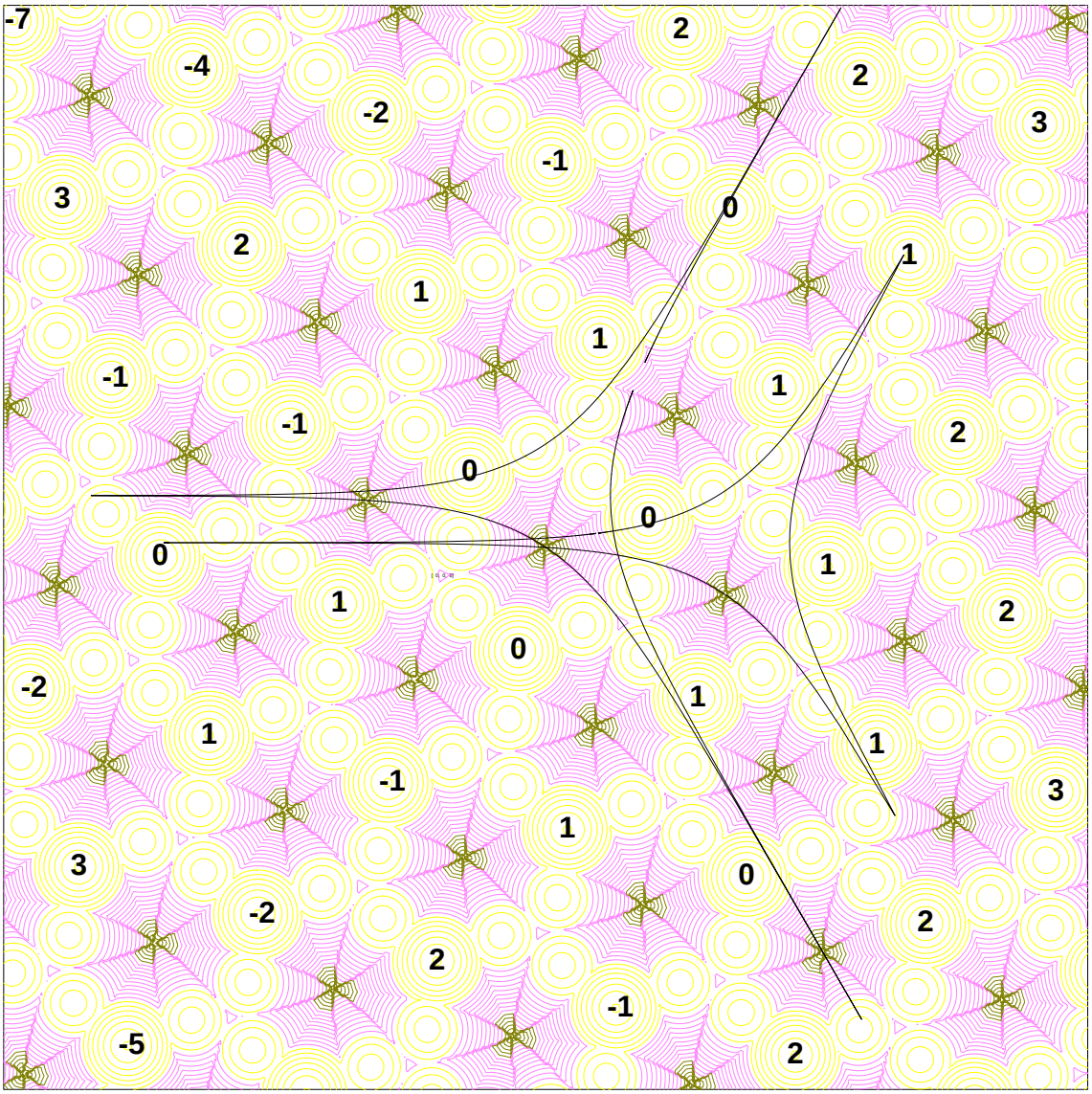

Figure 10. 'Tricorn' curves whose segments form hexad boundaries.

Z = -2

Y= 3	11	-5	6	1	7	8	15
Y= 2	4	-1	3	2	5	7	12
Y= 1	2	0	2	2	4	6	10
Y= 0	0	1	1	2	3	5	8
Y=-1	3	-1	2	1	3	4	7
Y=-2	-7	5	-2	3	1	4	5
Y=-3	22	-13	9	-4	5	1	6

Z = -1

Y= 3	12	-8	4	-4	0	-4	-4
Y= 2	4	-3	1	-2	-1	-3	-4
Y= 1	1	-1	0	-1	-1	-2	-3
Y= 0	1	-1	0	-1	-1	-2	-3
Y=-1	-2	1	-1	0	-1	-1	-2
Y=-2	6	-4	2	-2	0	-2	-2
Y=-3	-18	11	-7	4	-3	1	-2

Z = 0

Y= 3	15	-9	6	-3	3	0	3
Y= 2	5	-3	2	-1	1	0	1
Y= 1	2	-1	1	0	1	1	2
Y= 0	0	0	0	0	0	0	0
Y=-1	2	-1	1	0	1	1	2
Y=-2	-5	3	-2	1	-1	0	-1
Y=-3	15	-9	6	-3	3	0	3

Z = 1

Y= 3	18	-11	7	-4	3	-1	2
Y= 2	6	-4	2	-2	0	-2	-2
Y= 1	2	-1	1	0	1	1	2
Y= 0	1	-1	0	-1	-1	-2	-3
Y=-1	-1	1	0	1	1	2	3
Y=-2	4	-3	1	-2	-1	-3	-4
Y=-3	-12	8	-4	4	0	4	4

Z = 2

Y= 3	22	-13	9	-4	5	1	6
Y= 2	7	-5	2	-3	-1	-4	-5
Y= 1	3	-1	2	1	3	4	7
Y= 0	0	-1	-1	-2	-3	-5	-8
Y=-1	2	0	2	2	4	6	10
Y=-2	-4	1	-3	-2	-5	-7	-12
Y=-3	11	-5	6	1	7	8	15
X =	-3	-2	-1	0	1	2	3

Figure 11. Central portion of the infinite array of integers definining a particularly symmetrical specification of 'quasi-Fibonacci' numbers associated with the construction of generalized Fibonacci grids in four dimensions.